

Hippocampal Representation of Related and Opposing Memories Develop within Distinct, Hierarchically Organized Neural Schemas

Sam McKenzie,¹ Andrea J. Frank,¹ Nathaniel R. Kinsky,¹ Blake Porter,¹ Pamela D. Rivière,¹ and Howard Eichenbaum^{1,*}

¹Center for Memory and Brain, Boston University, Boston, MA 02215, USA

*Correspondence: hbe@bu.edu

<http://dx.doi.org/10.1016/j.neuron.2014.05.019>

SUMMARY

Recent evidence suggests that the hippocampus may integrate overlapping memories into relational representations, or schemas, that link indirectly related events and support flexible memory expression. Here we explored the nature of hippocampal neural population representations for multiple features of events and the locations and contexts in which they occurred. Hippocampal networks developed hierarchical organizations of associated elements of related but separately acquired memories within a context, and distinct organizations for memories where the contexts differentiated object-reward associations. These findings reveal neural mechanisms for the development and organization of relational representations.

INTRODUCTION

Recent research on the nature of memory representations in the hippocampus has emphasized a competition between pattern completion of a new experience to a previously stored representation versus pattern separation to an entirely novel representation in order to minimize interference between memory representations for similar events (Vazdarjanova and Guzowski, 2004; Deng et al., 2013; Colgin et al., 2010; Wills et al., 2005; Leutgeb et al., 2004; Lee et al., 2004; Bakker et al., 2008; Norman and O'Reilly, 2003; Hasselmo and Wyble, 1997). However, in direct contrast to this competitive mechanism that separates overlapping memories, an alternative view is that the hippocampus systematically organizes multiple overlapping memories to form relational networks, and these networks serve as knowledge structures, or schemas, that rapidly assimilate additional related memories (Eichenbaum, 2004; McKenzie and Eichenbaum, 2011; van Kesteren et al., 2010; Tse et al., 2007; Shohamy and Wagner, 2008; Zeithamova et al., 2012). A large literature supports the role of the hippocampus in relational representation and schema development, including studies in which intact but not hippocampal-damaged animals integrate overlapping memories (Dusek and Eichenbaum, 1997; Devito et al., 2010; Bunsey and Eichenbaum, 1996; Buckmaster et al., 2004; Tse et al., 2007) and complementary functional imaging studies in humans that

have identified hippocampal activation associated with successful integration of related memories (Wimmer and Shohamy 2012; Kumaran et al., 2009, 2012; Shohamy and Wagner 2008; Heckers et al., 2004; Greene et al., 2006; Zeithamova and Preston, 2010; Zeithamova et al., 2012; Poppenk et al., 2010; Preston et al., 2004; van Kesteren et al., 2010, 2012). Nevertheless, despite the established link between hippocampal function and relational representation and schema development, little is known about how neuronal populations in the hippocampus encode and organize related memories and whether and how pattern completion and separation mechanisms operate in these organizations.

Here we designed a task in which rats acquired memories that could be related in several ways including multiple features of events and where they occurred (Figure 1A). On each trial, rats entered one of two distinct spatial contexts and were presented with two objects located in either of two positions. In context 1, object A was rewarded, and not object B, whereas in context 2, object B was rewarded, not object A. Thus, the animals were required to use the spatial context to determine the appropriate object-reward associations. Previously, we have reported that single CA1 and CA3 neurons fire during stimulus sampling associated with multiple relevant stimulus dimensions, including object identity, location within a context, and context (Komorowski et al., 2009, 2013). Here we expanded the task to subsequently train the rats on an additional object set (C and D) within the same contexts. Following recent studies showing that high-dimensional neural representations in other brain areas can support complex cognitive functions (Ross et al., 2014; Rigotti et al., 2013), we employed a representational similarity analysis (Kriegeskorte et al., 2008) on simultaneously recorded hippocampal populations to reveal a hierarchical organization of distinct event and spatial features of the task, constituting the neural substrate of relational representation and schema structure.

RESULTS

Rats Acquire a Schema for Context-Guided Object Associations

To examine whether rats develop a capacity for rapid acquisition of new context-guided object associations, we trained a group of nonimplanted animals on three successive context-guided object association problems (Figure 1A). On the initial

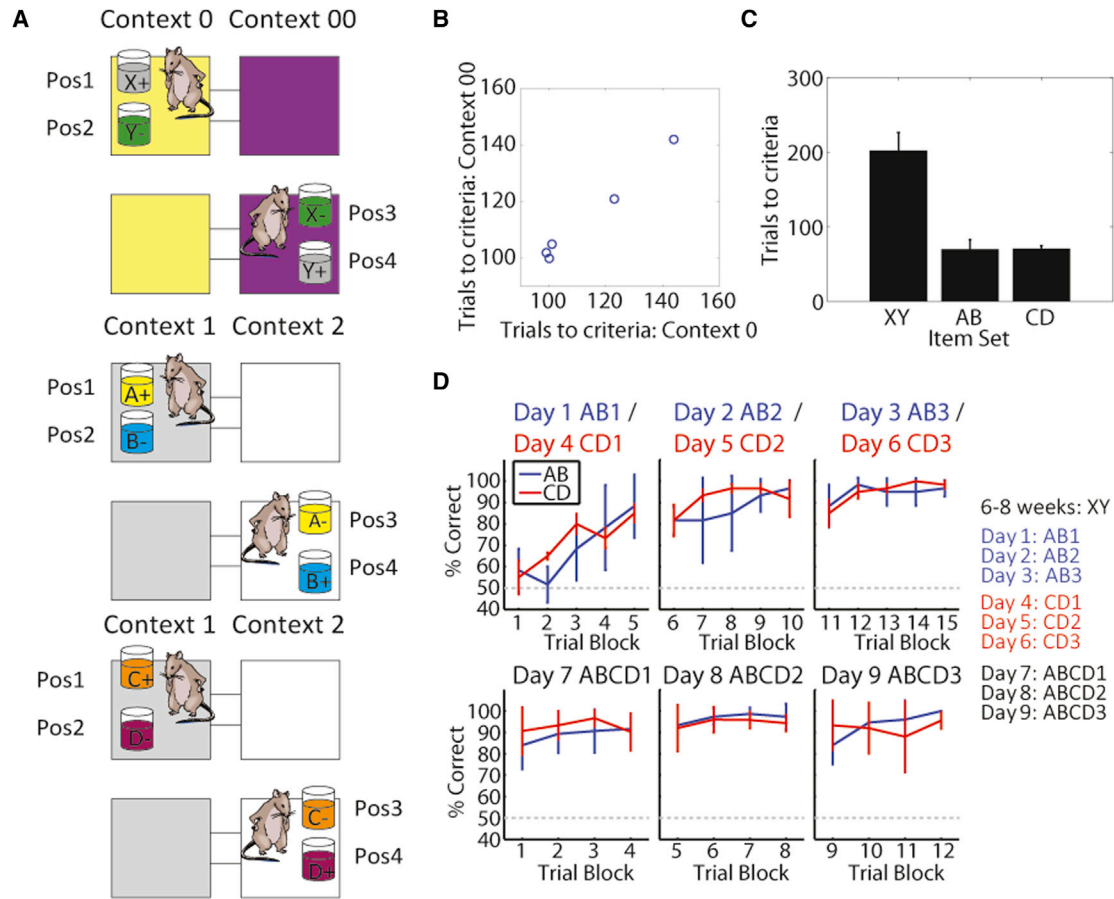


Figure 1. Rats Rapidly Learn Item and Context Associations

(A) Training protocol: rats initially learn problem set XY, then in a new pairs of contexts, problem sets AB and then CD.

(B) While learning XY, trials to criteria in context 0 was strongly correlated with that in context 00.

(C) After initial XY learning, rats rapidly acquired AB and CD.

(D) Performance across all 9 days of training. Rats performed above chance on AB by the fifth trial block on the first day of training (day 1: AB1). In contrast, rats performed above chance on CD on the second trial block on the first day in which those items were introduced (day 4: CD1). There were 15 trials per block. Error bars represent SEM.

problem (in context 0 choose item X; in context 00 choose item Y) rats performed better than chance (83% correct for 12 consecutive trials) in each context by 202 ± 23.8 trials over 7.0 ± 0.7 days (mean \pm SE). Learning curves for performance within each context were analyzed separately to determine the trial after which animals performed consistently above chance. The number of trials to criterion within each context was strongly correlated ($r = 0.995$, $p < 0.0004$, slope = 0.89; Figure 1B), suggesting that learning the opposing object-reward associations in the two contexts occurred around the same time.

Subsequently, rats were trained successively for 3 days on each of two object sets (AB and CD) within a new pair of contexts. With one exception, all rats reached the performance criterion for each set within a single day (trials to criterion 69.6 ± 13.1 for AB and 70.6 ± 3.8 for CD) and in significantly fewer trials than on the original set (mixed model repeated-measures ANOVA $F_{2,4} = 26.3$, $p = 0.003$; post hoc paired t tests; XY versus

AB $t(4) = 4.8$, $p = 0.008$; AB versus XY $t(4) = 6.6$, $p = 0.002$; AB versus CD $t(4) = 0.08$, $p > 0.05$; Figure 1C). These findings indicate that rats acquired a general schema for context-guided object association by the completion of an initial problem and could subsequently acquire new object sets rapidly. Notably, in the recording studies described below, implanted rats ($n = 5$) pretrained on the initial XY problem also subsequently learned AB and CD within a single session and performance remained high throughout testing on intermixed AB and CD sets (ABCD; Figure 1D).

Hippocampal Neurons Encode Multiple Dimensions of Item and Spatial Information

ANOVAs on firing rates of CA1 and CA3 neurons during object sampling on ABCD sessions identified firing patterns that differentiated item identities, item valence (rewarded or non-rewarded), co-occurrence of items within a set (AB or CD), position of item sampling within each context, and spatial

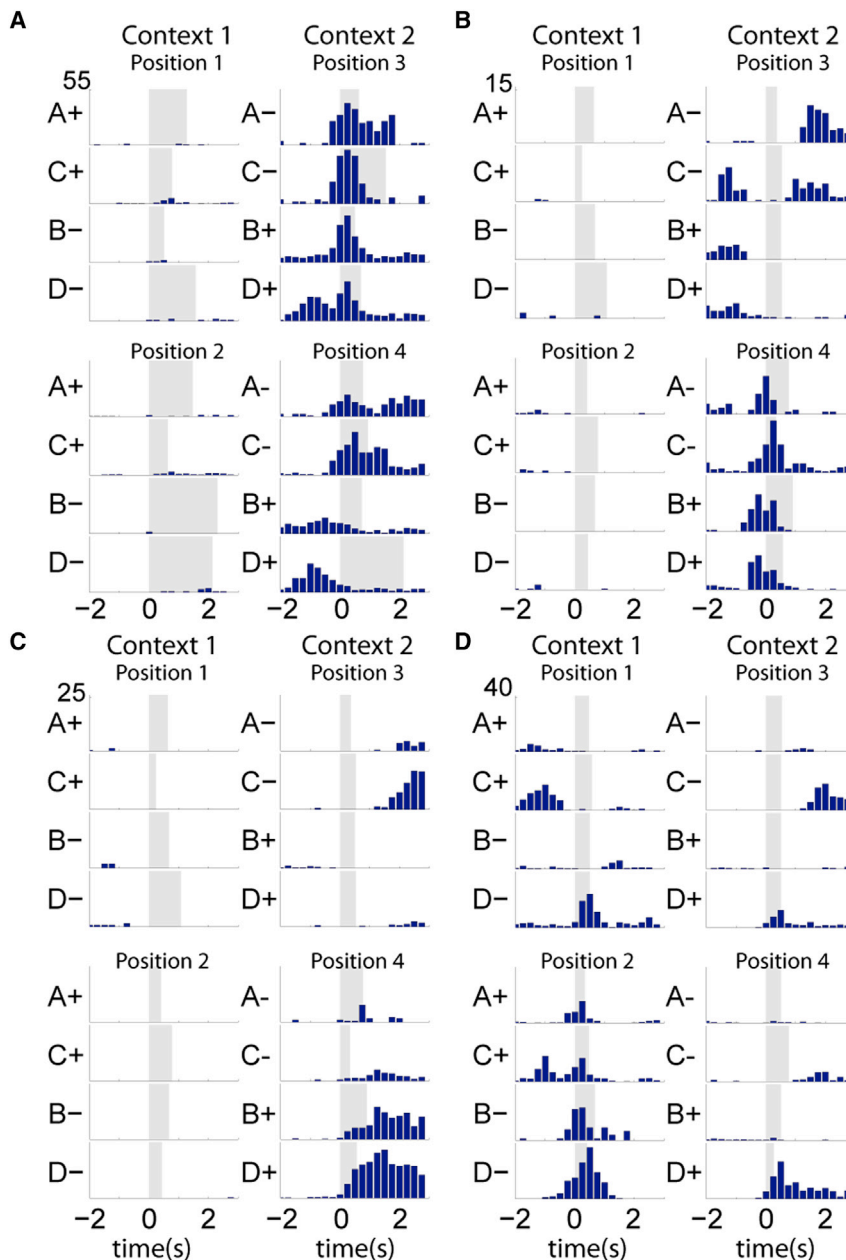


Figure 2. Example Responses from Hippocampal Cells during Item Sampling

Perievent time histograms (PETHs) centered on the onset of item sampling of example cells for the four items presented within each position. y axis is the trial average firing rate (Hz; scale at top left for each cell). Gray shading indicates the minimum sampling period. (A and B) CA3 neurons. (C and D) CA1 neurons. See also Figure S4 for histological confirmation of recording sites.

(Figure S1D available online). Therefore unless otherwise stated, we combined CA1 and CA3 cells to compose population firing rate vectors for each object sampling event.

Of the neurons whose activity was influenced by at least one variable, the firing rates of 79.7% neurons ($n = 244/306$) were also influenced by a combination of spatial (i.e., context and/or position) and object (i.e., set and/or valence) dimensions. For example, Figure 2A shows a neuron that fired at different rates during object sampling in the two contexts (greater activity in context 2) and its firing rate was also influenced by item valence (greater activity for nonrewarded items in position 4). Other neurons distinguished positions within a context (Figure 2B) with or without distinguishing rewarded from unrewarded objects (Figure 2C; position X valence interaction). Yet other neurons fired during object sampling at all positions, though at different rates for different items (Figure 2D; interaction of valence X set X position). A summary of the average firing rates for each item and place combination is shown in Figure 3A. Most cells fired at the highest rate during object sampling at one position and had a preferred item and/or valence within that position. Very few cells fired at equally high rates during sampling of all four

context. These analyses focused on the activity of 571 isolated neurons (CA1: 292, CA3: 279) during stimulus sampling epochs (mean duration = 1.53 ± 0.59 SD s). Based on a four-way (valence, set, position, and context) ANOVA for each neuron, the firing rates of 40.7% of the cells were influenced by context (CA1: 124, CA3: 109), 34.0% by position (CA1: 105, CA3: 90), 28.6% by valence (CA1: 84, CA3: 80), and 19.0% by set (CA1: 65, CA3: 43); and 13.5% of cells fired differentially depending on the interaction of valence and set, reflecting coding of item identity (CA1: 36, CA3: 39). These findings indicate that the firing patterns of individual neurons were modulated by multiple task dimensions and that equivalent proportions of CA1 and CA3 neurons were significantly influenced by each task dimension

items in the preferred position. Thus, the activity of individual hippocampal neurons reflects a multidimensional association of the relevant object and spatial dimensions that characterized this task.

Multidimensional Representational Similarity Analysis

To measure the similarity of ensemble representations of different item sampling events, we calculated the average z normalized firing rate for each neuron during all item sampling epochs and constructed a population vector for every sampling event based on these normalized rates. Examples of activity patterns of a simultaneously recorded ensemble taken from one recording session are shown in Figure 3B. The overall

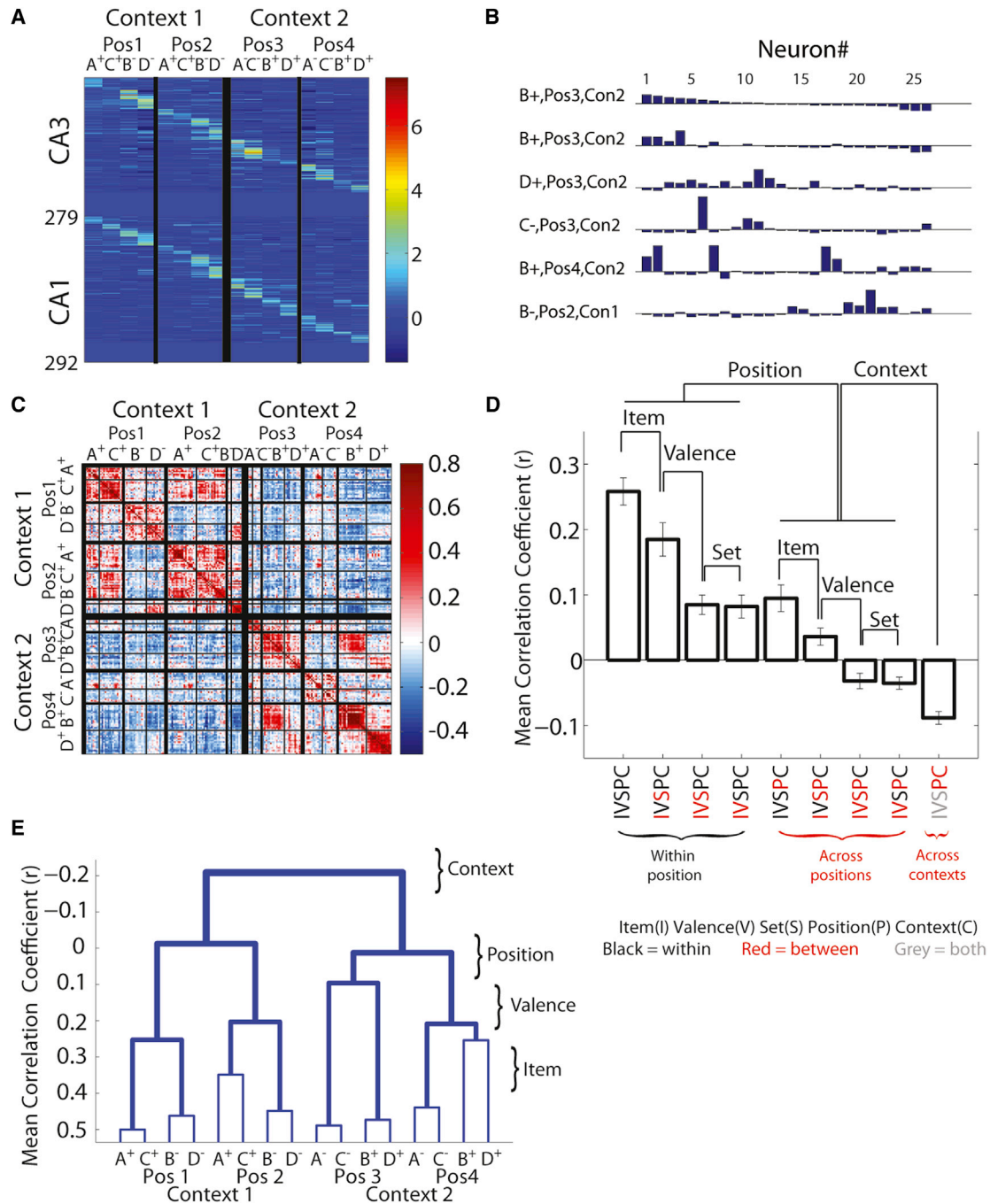


Figure 3. Ensemble Similarity Analysis Reveals Hierarchical Coding of Related Events

(A) Firing rates for all cells during ABCD, sorted for CA3 and CA1 by condition that elicited maximal firing rate. z axis is the trial averaged z normalized firing rate. x axis sorts trial types by context, position, valence, and item. Strong item coding is reflected in different firing rates among items within a position.

(B) Simultaneously recorded cell ensembles for seven trials within an example session. Each histogram is the population vector composed of Z scored (range -1.95 to 7.02 SD) firing rates during one trial identified by context (Con), position (Pos), item (A, B, C, D) and reward valence (+, -).

(C) An example correlation matrix from one session showing correlation coefficients by color code (right scale).

(D) The mean correlation coefficients (\pm SEM) for within- and between-condition item sampling events for each task dimension (see Table 1). For all dimensions except set, the correlation coefficients are higher for within-condition trials than between. IVSPC as defined in Table 1. See Figure S2 for individual rat data.

(E) A dendrogram showing that ensembles of the same valence in the same position are most similar, followed by ensembles associated with items of opposing valence within the same position. Positions within the same context were also coded more similarly than positions in the opposing context. See also Figures S1-S3.

Table 1. The Inclusion Filters for the within and between Conditions Whose Difference Operationally Defines Each Task Dimension

Task Dimension	Within Condition	Between Condition
Item within a position	IVSPC	IVSPC
Valence within a position	IVSPC	IVSPC
Set within a position	IVSPC	IVSPC
Item across positions	IVSPC	IVSPC
Valence across positions	IVSPC	IVSPC
Set across positions	IVSPC	IVSPC
Position	IVSPC	IVSPC
Context	IVSPC	IVSPC

Within-condition comparisons were those in which the ensemble activity from two sampling events were matched in the dimension of interest (e.g., from the same position). Between-condition comparisons were ideally identical to within-condition comparisons except for choosing two activity patterns recorded in conditions that differed only in the dimension of interest (e.g., from different positions). IVSPC is an acronym for each task dimension: I, item; V, valence; S, set; P, position; C, context. Black lettering indicates that recordings were from events of the same condition for that dimension (e.g., all black text indicates repetition of the same item in the same positions). Red lettering indicates that recordings were taken from events between conditions for that dimension (e.g., a red “P” indicates that ensembles were recorded during sampling events that occurred in different positions). Gray lettering indicates that recordings were taken from events both within and between conditions for that dimension.

ensemble pattern was similar for repetitions of sampling events with the same item in the same position (top two events). Ensemble patterns for events with different items of the same valence were partially overlapping; several new cells joined the ensemble, while others dropped out (top versus third events). Ensemble patterns for events with different valence in the same position showed more divergent firing patterns (top versus fourth event), and the overlap in the ensemble pattern decreased further still for events in different positions and in different contexts (top versus fifth and sixth events, respectively).

We created similarity matrices to visualize the patterns of ensemble similarity across all types of item-sampling events for each recording session. Figure 3C shows an example similarity matrix from one session in which item sampling events have been sorted by four task dimensions: item, valence, position, and context; set is not included because, as will be presented below, this dimension is not encoded by hippocampal ensembles. The similarity matrix shows that correlations between hippocampal population vectors for different sampling events reflect the identified task dimensions. For example, in this similarity matrix, in the top left corner ensemble patterns of items A+ and C+ are strongly correlated, showing representational similarity of items that have the same valence in the same position. Along the left column, ensemble patterns for A+ and C+ are strongly correlated between positions 1 and 2, showing similarity in representations of these items across positions in the same context. By contrast, looking further down the left column, ensemble patterns for A+ and C+ in position 1 are inversely correlated with those of the items in positions 3 and 4, showing anticorrelations in the alternate context.

To quantitatively compare the similarity of ensemble representations associated with these dimensions, we computed population correlation coefficients by combining the similarity matrices taken from each ABCD session of all subjects. We calculated mean population correlation coefficients for item, valence, and set dimensions within a position as well as across positions within a context, and for the combination of all comparisons across contexts (see Table 1 middle column for inclusion criteria). These analyses revealed modest but reliable correlation coefficients between population firing rate vectors between individual pairs of brief object sampling events (Figure 3D). For example, correlations between population firing rates during events with the same item in the same position had an average correlation coefficient of $r = 0.25$, but the SE of the mean across rats ($N = 5$) was only ± 0.02 , indicating that the variability of population firing patterns is highly consistent between identical individual events (Figure S2). Next, using the pooled correlations from every session (three per rat), we calculated a d' metric to measure the separation of the distributions of the correlation coefficients from specific conditions (e.g., pairs of identical sampling events) versus zero or versus the distribution of coefficients from an appropriate opposing condition (pairs of sampling events for the same item in different positions within the same context; see Table 1). The d' metric was compared against a bootstrapped data set to estimate the probability of the observed score against a random distribution. Despite the modest correlations, the observed correlation coefficients for each dimension were significantly different from zero (see Experimental Procedures, $p < 0.0001$). We also performed this analysis on the data pooled over three sessions for each rat, and the pattern of findings on each subject are similar to those for the combined data described below (Figures S2D and S2E). Parametric comparison of the mean correlation coefficients using each rat as the unit of analysis also revealed the same overall pattern (Figure S2D).

To measure the extent to which ensembles encoded each dimension, we compared the correlation coefficients within and between conditions of that dimension (for specific comparisons, see Table 1, middle versus right columns). Coding of item identity was measured by comparing ensemble correlation coefficients between population firing patterns during item sampling events with the same item in the same position to those with different items of the same valence at the same position (Figure 3D; Figure S2). Correlation coefficients for identical events (mean $r = 0.25$) were greater than those for events with different items of the same valence (mean $r = 0.18$; $d' = 0.23$, $p < 0.0001$), providing strong evidence that hippocampal ensembles differentiate items at specific locations. To measure coding of reward valence, we compared ensemble correlation coefficients among events that involved different items of the same valence to those that involved different items of different valences at the same position. The similarities of ensemble patterns for events involving different items with the same valence were greater than for events with different items of different valence (mean $r = 0.08$; $d' = 0.34$, $p < 0.0001$), indicating strong evidence that hippocampal ensembles differentiate items by valence at each location. To measure coding of sets (AB and CD), we compared ensemble correlation coefficients among

events that involved different items from the same set versus different items across sets at the same position. The similarities of ensemble patterns for events involving the item from the same and different sets were equivalent (within set mean $r = 0.08$; between set mean $r = 0.08$), indicating that hippocampal ensembles do not represent co-occurrence of items within sets ($d' = -0.02$, $p = 0.20$) any greater than their differentiation of item identity and reward valence.

To measure ensemble coding of positions within a context, we compared the ensemble correlation coefficients of sampling events that occurred within the same position to the correlation coefficients of ensembles that occurred in different positions within the same context (Table 1; Figure 3D; Figure S2). Ensemble patterns for events occurring within the same position were more similar (within position mean $r = 0.15$) than those across positions (mean $r = 0.02$; $d' = 0.45$, $p < 0.0001$), reflecting the well-known place code. However, the pattern of similarity across positions highly depended upon the items sampled in those positions. Pairwise comparisons of population correlation coefficients for sampling events with the same item in the two positions within a context showed the highest similarity (mean $r = 0.09$), as suggested by the observation that some cells fire in response to the same item presented in multiple locations (see Figure 2D; Wood et al., 1999). Activity recorded during events in which rats sampled the same item in different positions were more correlated than events in which rats sampled different items of the same valence (mean $r = 0.03$; $d' = 0.22$, $p < 0.0001$), which in turn were more correlated than sampling events that differed both by item identity and by the valence of those items (mean $r = -0.03$; $d' = 0.25$, $p < 0.0001$). Activity associated with items from the same set across positions were not more correlated than items from different sets across positions ($d' = -0.02$, $p = 0.15$), again showing the lack of differentiation of items between sets. Combining these observations, item identity and valence were coded both within a position and across positions, results that strongly argue against a model in which nonspatial information is coded only by the firing rate within single spatial firing fields (Leutgeb et al., 2005).

Finally, hippocampal patterns were anticorrelated between the two contexts (between context mean $r = -0.09$, probability of the observed correlations less than zero < 0.0001 ; Figure 3D), and the ensemble correlations for events that occurred in different contexts were significantly lower than the correlation of ensembles recorded in different positions within the same context (Table 1; $d' = 0.39$, $p < 0.0001$), indicating that contexts that define opposite item valence are associated with distinct patterns of neural activity.

This combination of results indicates a hierarchy of ensemble similarity during item sampling events. To illustrate this hierarchy, we constructed a dendrogram in which each item and position combination ($n = 16$) was associated with a population firing rate vector from neurons ($n = 560$) across all sessions and all rats. These population vectors were correlated and vectors that produced the largest correlations were grouped into clusters (see Experimental Procedures). This analysis shows that the highest average similarity of ensemble patterns for item sampling events of the same valence in the

same position, followed by events of opposite valence in the same position, followed by events in the other position within the same context, and finally, the anticorrelation for events that occurred in the alternate context where items had opposite reward contingencies (Figure 3E). There are a larger number of possible dendrograms ($C_{15} = 9,694,845$) and therefore the likelihood of observing this particular binary tree by chance is low.

We confirmed these results by estimating the probability that a pattern of ensemble firing rates was recorded in each of the 16 item in position combinations using a Bayesian decoding algorithm. The decoding algorithm generated the same hierarchy of ensemble similarity as the correlational techniques described above (Figure S3). Ensembles were most likely to have been recorded from the correct item and position combination (mean probability = 0.38), which was greater than the probability of the unit activity originating from trials with a different item of the same valence in the same position (mean probability = 0.18; $d' = 0.58$, $p < 0.0001$). This significant difference in probability reflects the strong item coding. The next most likely origin of the recorded ensemble was from sampling events occurring in the same position though containing an item of opposing valence (mean probability = 0.05, $d' = 0.48$, $p < 0.0001$). This significant difference in probability reflects the valence code. Ensembles were equally likely to originate from sampling events of the same set (mean probability = 0.05) as from samples of the other set (mean probability = 0.04), confirming the lack of a distinct code for item pairing ($d' = 0.08$, $p = 0.15$). The position code was reflected by the higher probability that ensemble activity was recorded in the correct position (mean probability = 0.20) than the probability of being recorded in the incorrect position within the correct context (mean probability = 0.06; $d' = 1.24$, $p < 0.0001$). Finally, ensembles were least likely to have been recorded in the opposing context (mean probability = 0.02), with a mean probability of decoding to the wrong context lower than decoding to the wrong position within the same context ($d' = 0.38$, $p < 0.0001$) and lower than decoding to the opposing context by chance ($p = 0.0013$).

Based on these results, we conclude that item identities, their reward valences, and the locations where items appear within a context are encoded by hippocampal ensembles during item sampling. Notably, the co-occurrence of items within a set is not encoded by hippocampal ensembles in the current task. Finally, hippocampal ensembles strongly separate representations of events in different contexts, suggesting opposing schemas are created for events in contexts that are meaningfully distinct.

Both CA1 and CA3 Encode Item and Spatial Dimensions

Different functions have been ascribed to areas CA1 and CA3 (Farovik et al., 2010; Hoge and Kesner, 2007; Lee et al., 2004; Leutgeb et al., 2004; Hasselmo and Wyble, 1997; Alvernhe et al., 2008; Dupret et al., 2010; Rolls, 2013), and therefore we tested whether these two hippocampal regions differentially coded each of the task dimensions. Population firing rate vectors were computed separately for simultaneously recorded CA1 and CA3 ensembles (Figure S4) and the correlational analyses

described in the previous section were repeated for these region-specific ensembles (Figures S1A–S1C).

In both regions, when analyses were limited to item sampling events that occurred within the same position, events in which the item identity were matched were better correlated (CA1: $r = 0.23$, CA3: $r = 0.34$) than events in which different items of the same reward valence were presented (CA1: $r = 0.15$, $d' = 0.23$; CA3: $r = 0.29$, $d' = 0.11$; $p < 0.0001$ for both regions). Changing both item identity and reward valence caused further decreases in ensemble correlation coefficients in both regions (CA1: $r = 0.09$, $d' = 0.19$; CA3: $r = 0.21$, $d' = 0.19$; $p < 0.0001$ for both regions). Therefore, firing rates of cells in areas CA1 and CA3 are influenced by item identity and reward valence of items that occupy a single position.

Comparisons of firing rates recorded within the same positions revealed that area CA3 but not CA1 showed higher population correlation coefficients for events containing items of the same set (CA1: $r = 0.09$, CA3: $r = 0.22$) than for items of separate sets (CA1: $r = 0.08$, $d' = 0.03$, $p = 0.24$; CA3: $r = 0.20$, $d' = 0.04$, $p = 0.002$). This difference between regions was observed when comparing two distributions of correlation coefficients (same set versus different set) composed of observations pooled across rats. Significance testing for each rat revealed set coding in only a single subject ($d' = 0.10$, $p < 0.001$), suggesting that any item set code in area CA3 is secondary to the representation of other task dimensions.

Both regions showed higher correlation coefficients for sampling events that occurred within the same position (CA1: $r = 0.14$, CA3: $r = 0.27$) than for samples that occurred across positions within the same context (CA1: $r = 0.01$, $d' = 0.35$; CA3: $r = 0.12$, $d' = 0.36$; $p < 0.0001$ for both regions). The correlation of activity patterns recorded within a context were higher in both regions than correlations for samples that occurred in the opposing contexts (CA1: $r = -0.06$, $d' = 0.23$; CA3: $r = -0.03$, $d' = 0.34$; $p < 0.0001$ for both regions), which were significantly anticorrelated in both regions ($p < 0.0001$ for both regions). Thus, the full schema that was identified when ensembles were pooled between the two hippocampal fields existed in both CA1 and CA3.

To determine whether a particular task dimension (e.g., position) had a stronger influence on population firing patterns in CA1 versus CA3, the degree of dimensional coding was estimated with a d' metric described above. The difference between the d' metrics calculated for each region was compared against a randomized data set in which the identity of each neuron (CA1 or CA3) was shuffled 10,000 times. Position, context, set, and valence were coded similarly by these regions (the probability that the observed difference between d' metrics was larger than shuffled data was greater than 0.2 for each dimension) (Figure S1C). In contrast, CA1 showed greater item coding for sampling events that occurred within a position (CA1 $d' = 0.23$; CA3 $d' = 0.11$; $p = 0.003$) and also showed greater item coding when activity patterns were compared across positions within the same context (CA1 $d' = 0.25$; CA3 $d' = 0.08$; $p < 0.0001$). Therefore, while item information influenced firing rates in both regions, CA1 ensembles distinguished items within a fixed position as well as across positions more so than CA3 ensembles.

Nonspatial and Spatial Dimensions Are Distinctly Expressed during Item Sampling

We next explored whether different dimensions of an event are encoded as a unified representation, or whether each dimension is encoded distinctly, consistent with an associative network of the component elements of memories. We reasoned that, if an item's identity, valence, and position are integrated within a unified representation, they should all be expressed simultaneously. On the other hand, if these dimensions are distinctly encoded, then their representations might be expected to appear sequentially during the item-sampling period. To address this question, firing rates for each item-sampling event were calculated for 250 ms bins centered around the onset of item sampling and ensembles recorded on different samples were correlated at each time bin.

These analyses indicated that information about item identity, valence, and position are expressed sequentially rather than simultaneously. Position information was expressed first. For all types of item sampling events that occurred within the same position, at the outset of sampling there was an initial increase in the mean ensemble correlation regardless of whether the sampling events contained the same item (Figure 4A, black), different items of the same valence (Figure 4A, red) or different items of opposing valence (Figure 4A, green), indicating a reliable position code at the onset of sampling. In contrast, ensemble correlations between positions were, on average, low throughout item sampling (Figure 4A, gray). The difference between the within position versus between position correlations was assessed using the d' metric that reflects the degree of position coding (Figure 4B, gray). Position d' was significant for approximately 1,000 ms before item sampling and peaked 250 ms after item sampling before significantly decreasing (max $d' - \min d' = 0.19$, probability observed d' range in bootstrap data < 0.001) (Figure 4B, gray).

The decrease in position coding was caused by the onset of item and valence coding that increased the variability of firing within a position. For sampling events with the same item in the same position, the average ensemble correlation increased upon arrival to the items and remained high throughout item sampling (Figure 4A, black), indicating reliable coding throughout the sampling epoch. Sampling events with different items of the same valence (Figure 4A, red) showed the same initial increase in ensemble correlation, which subsequently decreased throughout item sampling, reflecting the divergence of neural firing patterns in response to different stimuli—the item code. The d' metric for item coding (Figure 4B, black) was statistically significant from the onset of sampling until the reward was retrieved and peaked 1,000 ms after item sampling. Therefore, item information increased at the same time points when position coding decreased.

Valence information influenced hippocampal neuronal firing rates last during item sampling. When comparing samples with different items and different reward valence (Figure 4A, green), neural activity was initially well correlated, reflecting the position code. However, 750 ms after item sampling, ensembles recorded during events with different items of the same valence were significantly more correlated than ensembles recorded during samples of items with different valence, as shown by

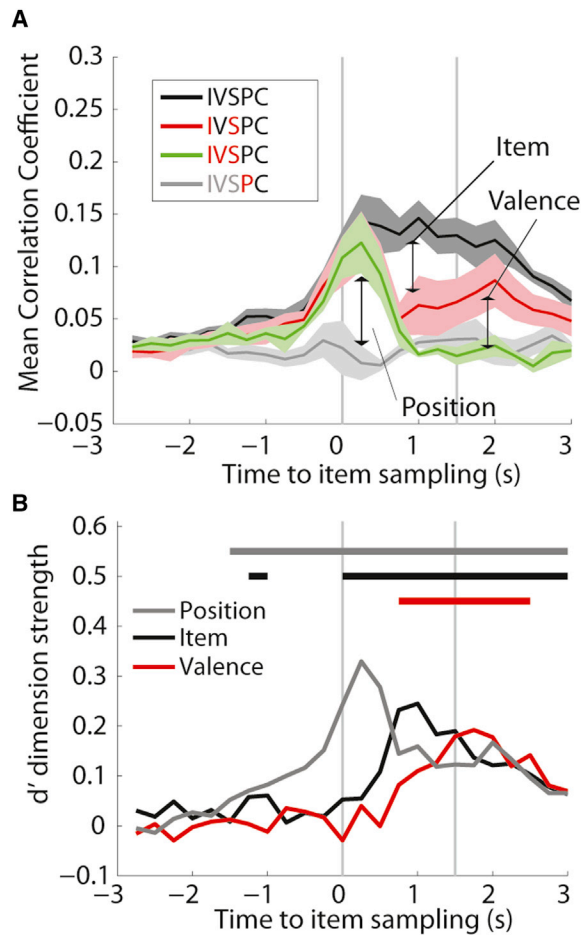


Figure 4. Task Dimensions Are Expressed at Different Times during Item Sampling

During item sampling, position is coded first, followed by item, and finally valence.

(A) The ensemble correlation analyses was done using the population firing rates taken from 250 ms bins centered around sampling for trials in the same location. Sampling epochs shorter than 1.5 s were excluded. IVSPC defined in Table 1. Mean of each rat's average correlation coefficient is plotted with SEM ($N = 5$).

(B) The average d' for item (black) and valence (red) and position (gray) for trials in the same position. Color coded bar above graph shows periods in which that dimension was significantly coded.

the increase in the valence d' metric at these times (Figure 4B, red). Notably, valence coding peaks at the end of the item sampling period, suggesting this activity may reflect preparation of the differential behavioral response associated with items of opposite valence.

The distinct representation of position, valence, and item coding suggests that these task dimensions are encoded as distinct elements rather than unified conjunctions.

New Associations Are Rapidly Assimilated within the Existing Hippocampal Network

A defining property of schemas is that new memories are stored within the structure of related existing memories (Piaget,

1928; McKenzie and Eichenbaum, 2011; McClelland et al., 1995; McClelland, 2013). Therefore, we tested the hypothesis that neural activity recorded during training of the second item set (CD) would be similar to activity already established during training on the first item set (AB) learned within the same context. We expected a stable position and context code, because adding new items within the same spatial organizations did not alter the meanings of these task dimensions. Also, based on the view that schemas link closely related events, we also expected similarity in the ensemble representations of items that similarly predict reward or nonreward within a context.

To determine whether firing patterns reflected the similarity of the two item sets, we first identified the item and position conjunction that generated the highest firing rate during the last day of training on the first item set (AB3; see Figures 1A and 1D). We then used this preferred item and position for each neuron to compare firing rates during sampling of items of the same and different valence during the first day of training on the second item set (CD1). This required comparing the activity patterns of the same neurons between two successive daily sessions, and so this analysis focused on 38 neurons that were carefully selected as having identical characteristics across days (see Experimental Procedures). As predicted, we observed that in 52.6% of the cells ($n = 20/38$), the median firing rate recorded during the second item set was higher for the same-valence item in the preferred position than in any of the other seven item and place combinations ($\chi^2 = 52.4$, $p = 4.65 \times 10^{-13}$). For example, cell 1 in Figure 5A fired for unrewarded item B— in both positions in context 1 and fired equivalently for unrewarded item D— in both positions in context 1 (main effect valence $F(1,213) = 16.96$, $p = 0.0001$, item B versus item D in positions 1 and 2, $P_s > 0.05$). Similarly, cell 2 showed equivalent firing for unrewarded items A— and C— in only one of the positions in context 2 (main effect valence $F(1,213) = 171.1$, $p < 10^{-28}$; item A versus item C in position 3, $t(8) = 0.33$, $p = 0.75$).

To examine when common firing across item sets emerged, we compared firing rates on the first and last encounter with each new item (items C and D) for which animals made the appropriate behavioral response. On both the first and last sampling event, firing rates were higher in the preferred positions (mixed-model repeated-measured ANOVA, main effect position $F_{1,37} = 10.68$, $p = 0.002$, post hoc t tests at each time point, $P_s < 0.05$), revealing a stable position code across item sets. Even on the first correct encounter with each item in the preferred position (absolute sample number 1–48, mean sample number = 11.25 ± 11.86 SD), there was a trend that cells fired more for the same-valence item (mean Z score rate = 1.24 ± 0.35) than the different-valence item (mean Z score rate = 0.38 ± 0.28 ; paired t test, $t(37) = 1.99$, $p = 0.053$) (Figure 5B, first sample), though an equal number of cells fired maximally to the same ($n = 20/38$) and different valence items ($\chi^2 = 0.02$, $p = 0.87$). By the end of training, cells clearly showed a firing rate preference for the equivalent item. On the last sampling events for each item in the preferred position, cells fired at a significantly higher rate for same-valence items (mean Z score rate = 1.17 ± 0.31) as compared to items of opposing valence (mean Z score rate

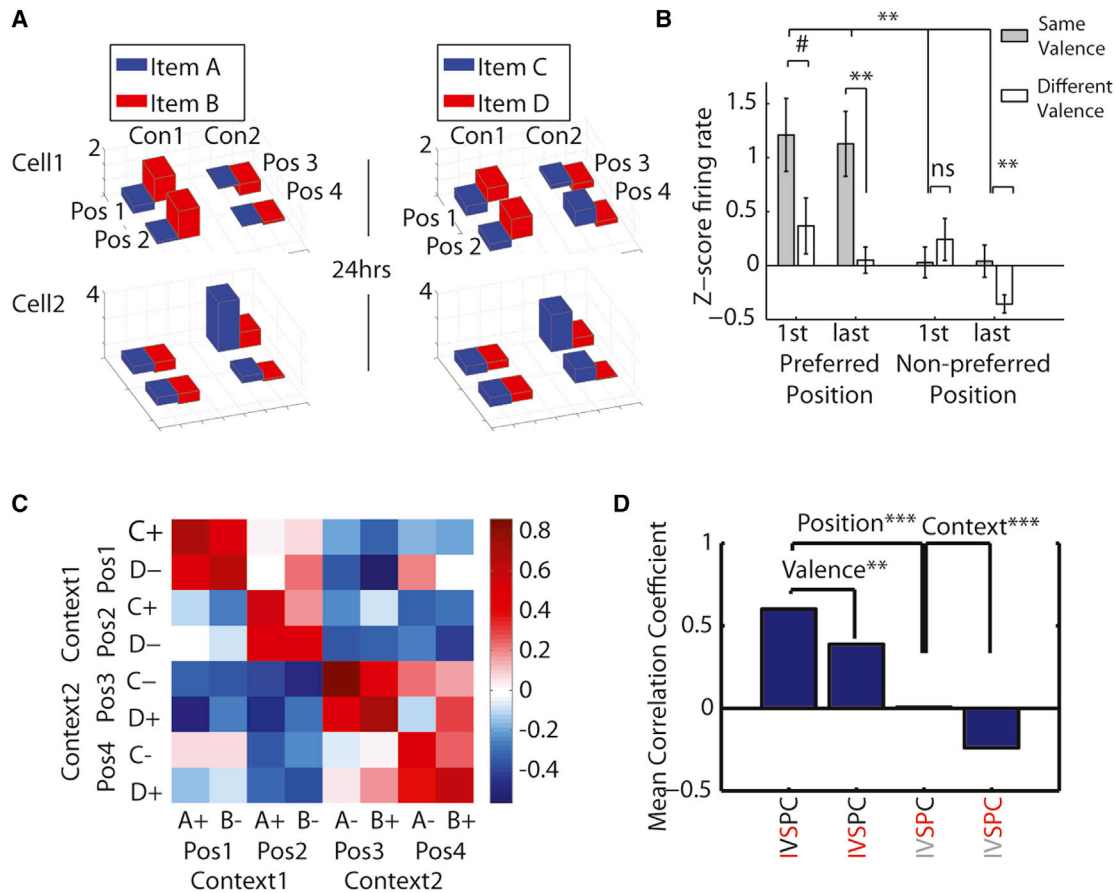


Figure 5. New Items Are Encoded within an Established Schema

(A) The Z score firing rate for two cells recorded on the last day of training on the first item set (AB3) and the first day of training on the second item set (CD1) 24 hr later.

(B) The mean Z score firing rate recorded on the first and last encounter with each item, as identified on AB3 training. Error bars represent SEM.

(C) Data from AB3 and CD1 were merged and the median ensemble rates for each item and place conjunction were calculated and population vectors were correlated from AB3 to CD1 to create the 8×8 similarity matrix.

(D) The valence, position and context coding that developed over AB training was preserved and extended to training with the new item set. IVSPC defined in Table 1. # $p = 0.053$, * $p < 0.05$, ** $p < 0.01$, *** $p < 0.0001$. See also Figure S5.

0.11 ± 0.13 , $t(37) = 3.52$, $p = 0.001$) (Figure 5B, last sample) and far more cells ($n = 33/38$) fired maximally to the equivalent item ($\chi^2 = 19.2$, $p < 0.00001$).

We then tested for differences in firing to the same- and different-valence items in the nonpreferred location within the preferred context. On the first sample with each item, there were no differences in firing rates ($t(35) = 1.47$, $p = 0.15$), though by the final sample there was greater firing to same-valence items ($t(35) = 2.81$, $p = 0.008$) (Figure 5B, nonpreferred position). These results show that during learning, cells developed a preference for the item of the same valence in both the preferred and nonpreferred positions.

We next asked whether the overall neural representation developed during training of the first item set was reinvoked during training of the second item set. We adopted a similar correlation analysis as that previously described for analyzing days when all items were intermixed, though instead of comparing

simultaneously recorded ensembles on individual samples, we calculated the median firing rate for each item and place combination (four items in four positions) for each cell ($n = 38$) and concatenated these rates across rats for subsequent analysis. The ensemble similarity in response to different item and position combinations was established by examining the correlations of cell activity recorded at every item and position combination for the first item set (two items in four positions) with firing rates recorded during initial training of the second item set (two new items in the same four positions) recorded 24 hr later. The resulting 8×8 similarity matrix describes which item and position combinations result in overlapping hippocampal ensembles (high correlations) and therefore operationally defines the neural network organization of the task dimensions (Figure 5C). As suggested by the findings on single-cell activity patterns, when analyses were limited to sampling events occurring in the same position, samples with different items of

the same valence were more correlated (mean $r = 0.60$) than samples with different items of opposing valence (mean $r = 0.38$; $d' = 1.79$, $p = 0.001$), suggesting a subset of cells that fired during the first item set fired similarly for the equivalent item of the second item set.

We also found evidence for a stable position and context code. Population activity patterns recorded during item sampling in the same position across days were more correlated (mean $r = 0.49$) than those recorded in different positions (mean $r = 0.02$; $d' = 3.06$, $p < 0.0001$), which were in turn more correlated than those recorded within the other context (mean $r = -0.24$; $d' = 1.84$, $p < 0.0001$) (Figure 5D). Together, these data show that neural correlates of the entire task structure that developed during training on the first item set were adopted and extended to encode related items that occurred within the same context.

The combined findings in these analyses suggest that neural activity during learning of new item associations reflected binding of information acquired over multiple days into a unified schema that represents equivalent item and position associations within overlapping hippocampal networks. The item and place conjunctions that generated correlated neural activity at the end of learning both item sets were qualitatively the same as those observed during overtraining days in which all items were presented, suggesting that the schema that developed during learning was maintained until the final day of behavioral testing.

DISCUSSION

The present findings show that hippocampal neuronal networks represent a hierarchical organization that links overlapping elements of related memories. For both spatial and nonspatial elements of separate experiences, related features were integrated within an organized representation, whereas events that dictated divergent behavior and reward expectations were separated into distinct hippocampal representations. These findings show that memory representations in the hippocampus are not characterized by unified configurations of places identified by specific landmarks, but rather that the hippocampus creates a schematic representation of the behaviorally relevant relationships between distinct elements of memories, including perceptually defined objects, their meaning, and the places they occur, and strongly separate schemas are created for events that occur in meaningfully different contexts.

These results add to a confluence of evidence indicating that the hippocampus encodes both nonspatial and spatial features of an experience. Several studies have reported that hippocampal neurons respond to specific nonspatial stimuli only within the place field for each cell (Komorowski et al., 2009; Moita et al., 2003), while others have reported responses to common stimuli across multiple locations (Wood et al., 1999; Manns and Eichenbaum, 2009; McKenzie et al., 2013; Singer et al., 2010; Eichenbaum et al., 1987). We observed both types of responses as shown by item and valence coding within and across positions. Some have hypothesized that spatial contexts are represented by qualitatively distinct mappings of place cells, whereas events are encoded by quantitative differences in firing rate (Leutgeb

et al., 2005). The present findings indicate a more complex, yet highly organized population representation in the hippocampus that interleaves distinct and related events within and across positions and contexts.

We observed that most CA1 and CA3 neurons exhibited high-dimensional coding, including conjunctive responses to both object and spatial dimensions (Komorowski et al., 2009; Manns and Eichenbaum, 2009; Anderson and Jeffery, 2003; Wiebe and Stäubli 1999; Deshmukh and Knierim, 2013), consistent with the convergence of the “what” and “where” pathways within the hippocampus (Witter et al., 2000). The importance of associating events and the places and context in which they occur is prominent in studies of hippocampal memory function in animals (Balderas et al., 2008; Komorowski et al., 2013; Tse et al., 2007; Parkinson et al., 1988) and humans (Holdstock et al., 2002; Vargha-Khadem et al., 1997). Together, these results and others (Davachi et al., 2003; Diana et al., 2010) support the hypothesis that the hippocampal contribution to memory involves binding of items within a contextual framework (Eichenbaum et al., 2007; Diana et al., 2007).

Many have argued that the binding of items in contexts increases the uniqueness of memory traces, allowing the storage and recollection of distinct episodic memories (Gilbert et al., 1998; Yassa and Stark, 2011; Norman 2010; Norman and O'Reilly 2003; Xu and Südhof, 2013; Hasselmo and Wyble, 1997). The observation that place cells generate independent spatial mappings in different contexts (Paz-Villagrán et al., 2004; Spiers et al., 2013; Leutgeb et al., 2004; Kubie and Ranck 1983; Hayman et al., 2003) has suggested that the hippocampus creates qualitatively distinct representations of overlapping memories in order to reduce interference (Kumaran et al., 2012). Challenging this view, here we found strong evidence that similar events are represented within a hierarchical organization of correlated hippocampal firing patterns.

Other recording studies have suggested elements of a common hippocampal code for related events. When animals perform the same behavioral response to retrieve a reward at different positions, subsets of hippocampal neurons fire similarly at multiple locations around a circular track (McKenzie et al., 2013). Similarly, when animals traverse parallel arms of a W-shaped maze to retrieve reward, cells fire at equivalent positions on each arm, suggesting a common code for functionally equivalent events at different locations (Singer et al., 2010). In humans, monkeys, and rats, hippocampal neurons respond to categories of items that are functionally equivalent (Kreiman et al., 2000; Quiroga et al., 2005; Deadwyler et al., 1996). These parallel lines of evidence indicate that the hippocampus records common features of events within overlapping networks that link related memories (Eichenbaum, 2004). Furthermore, whereas other studies have reported differences in continuous versus categorical coding in CA1 and CA3 (Leutgeb et al., 2004; but see Colgin et al., 2010), respectively, here neuronal networks across these areas act cooperatively in a common, continuous, and hierarchical organization of memory representations.

Importantly, the hippocampus did not similarly encode sets of items that co-occurred within trials throughout training. This finding is striking for several reasons. First, it is notable that rats move rapidly between objects within trials, such that

pairs of sampling events with items of the same set were on average presented much closer in time than items between sets. The absence of strong correlations despite these shorter intersample intervals indicates that high correlations between items of the same valence from different sets were not due to baseline temporal correlations in hippocampal cell firing. Second, these results are an important control showing that the hippocampus does not code all possible regularities but only those that are meaningful, in this case, stimuli that have in common that they predict reward or nonreward. Third, several models strongly predict that events that occur closely in time will be represented by correlated patterns of activity due to the recall of the common temporal context (Howard and Kahana, 2002). The current results do not necessarily indicate that the hippocampus does not encode temporal context but do suggest that in the present paradigm, common temporal context is secondary to other meaningful regularities including spatial context, position, reward, and the perceptual properties of the sampled item. These findings indicate that hippocampal networks do not necessarily capture a unified and qualitatively distinct “snapshot” of each episode but rather the absence of a hippocampal code for co-occurrence reflects the integration of multiple related, albeit separate, experiences into a schematic organization.

We found that events that occurred in different contexts were represented by anticorrelated hippocampal population firing patterns. This finding is in contrast to the independent place code that is often reported for unrelated contexts and also distinct from observation of anticorrelated activity for different behaviors executed within the same space (Bahar et al., 2011; Markus et al., 1995). In our experiment, rats executed the same behaviors in both contexts, though in response to different items. Therefore, the anticorrelated representations reflect either the context-dependent item associations or the behavior and item associations but cannot simply reflect behavior or arousal alone (O’Keefe 1999). The additional finding of anticorrelated representations of events of opposite significance across locations within a context suggests that strong separation of representations may be driven by opposing significance of events within or between contexts.

Previous studies have established that place cells maintain a somewhat stable place code across days (Ziv et al., 2013; Thompson and Best, 1990; Mankin et al., 2012). We extend these findings and show that cells also maintain a stable valence code across days and across different items when training produces consistent behaviors across days. After characterizing the items that cells prefer, 79% of those cells went on to fire more in response to other items of equivalent valence. These results suggest that, at the time of learning, new information is rapidly assimilated within networks of related memory traces (Eichenbaum, 2004; McKenzie and Eichenbaum, 2011). Similarities in hippocampal coding between familiar and novel conditions probably reflects the integration of related memories, arguably a primary purpose of memory systems in schema development and memory consolidation (McClelland et al., 1995; Tse et al., 2007). This overlapping code at the time of learning builds relational representations that could support transitive associations between separately learned experiences via of their common

associations with a behaviorally relevant context (Dusek and Eichenbaum, 1997; Bunsey and Eichenbaum, 1996; Zeithamova and Preston, 2010; Zeithamova et al., 2012).

EXPERIMENTAL PROCEDURES

Subjects and Behavioral Task

Subjects were ten male Long-Evans rats kept on food restriction and held at a minimum of 85% free-feeding weight. All animal procedures were approved by the Boston University Institutional Animal Care and Use Committee.

The contexts were two chambers separated by a central alleyway that differed in terms of color and texture of the floors and wall. The objects (referred to as “items”) were terra cotta pots filled with different digging media (e.g., shredded paper) and scented with different essential oils (e.g., maple) and reward was a small bit of cereal buried in one of the pots. On each trial, two objects were located in either left-right spatial configuration within a context randomized across trials. After learning the initial XY problem, five rats were implanted with hyperdrives in dorsal CA1 and CA3 then, after surgical recovery and identification of neuronal activity, were trained successively on AB and CD for 3 days each, then for 3 days on both sets concurrently in randomly presented AB and CD trials (ABCD). Another set of five nonimplanted rats were used to measure learning rates on each problem.

Single-Neuron Analyses

For every item sampling event, cell firing rate was determined as the number of action potentials observed during at most 2 s of sampling. A four-way ANOVA was calculated for each cell’s firing rate with main effects of: context, position nested within context, valence, and item set. All interactions were also calculated and item coding was assessed through the interaction of valence and set (see Figure S1D for proportion of significant cells in CA1 and CA3).

Multidimensional Representational Similarity Analyses

Firing rates for individual neurons were Z score normalized using the mean and SD among all item sampling events to create a population vector of normalized rates for each event. The Pearson’s correlation coefficient of these population vectors was calculated for every pair of events. Strength of a coding dimension was calculated by comparing the mean correlation for events within versus between conditions for that dimension (Table 1). The dimension d' was generated either for individual rats or for the experiment as a whole by pooling the correlations among rats. The observed d' was compared to bootstrap data set in which event identities were shuffled 10,000 times and then the correlation analysis and d' metrics were recomputed for each bootstrap sample (Figure S2). When data were compared against zero, the d' metric was the mean correlation coefficient divided by the SD.

The hierarchical nature of the schema was visualized using the MATLAB R2012b functions linkage and dendrogram. For each item and position combination, a large firing rate vector was created composed of the median firing rates of every cell ($N = 560$) recorded from a session in which correct behavior was observed for all 16 item and place conjunctions (one session failed to meet this criteria) (see Figure 3E). The agglomerative hierarchical cluster tree was then created using the unweighted average distance between pairs of vectors and the Pearson’s correlation coefficient as the distance metric.

Temporal Dynamics of Population Firing Patterns

To assess when different dimensions emerged during item sampling, we ran a similar analysis though firing rates were taken at different 250 ms time bins centered ± 3 s around item sampling (Figure 4). Only events for which the rat’s head remained over the pot for over 1.5 s were included. Significance testing was done using the same bootstrap analysis at each time point and comparing whether the observed d' was significant at $p < 0.002$ (Bonferroni correction for 24 time points).

Comparison of Representations across Learning AB and CD Problems

The last day of AB training (AB3) was merged with the first day of CD training (CD1), to investigate how firing during sampling of A and B generalized upon

first introduction of C and D (see [Supplemental Experimental Procedures](#) for analyses to ensure recording stability and [Figure S5](#)). To assess the similarity of neuronal activity for one item set (e.g., AB) versus that for the other item set (e.g., CD), we associated each item and position combination ($n = 16$) with a firing rate vector composed of the rates of every cell ($N = 38$). The pairwise correlation of these vectors across days generated an 8×8 similarity matrix, which reflects the overlap in neural activity for each item and place combination. These correlations were grouped and averaged to compare task dimension coding as described above. Statistical testing was done by shuffling the item/position identity of each median rate vector and recalculating the correlations on the randomized data set.

SUPPLEMENTAL INFORMATION

Supplemental Information includes Supplemental Experimental Procedures and five figures and can be found with this article online at <http://dx.doi.org/10.1016/j.neuron.2014.05.019>.

ACKNOWLEDGMENTS

We greatly appreciate the productive conversations with Marc Howard throughout the preparation of this manuscript. This work was supported by NIMH MH52090, MH094263, and ONR MURI N00014-10-1-0936.

Accepted: April 30, 2014

Published: June 5, 2014

REFERENCES

- Alvernhe, A., Van Cauter, T., Save, E., and Poucet, B. (2008). Different CA1 and CA3 representations of novel routes in a shortcut situation. *J. Neurosci.* *28*, 7324–7333.
- Anderson, M.I., and Jeffery, K.J. (2003). Heterogeneous modulation of place cell firing by changes in context. *J. Neurosci.* *23*, 8827–8835.
- Bahar, A.S., Shirvalkar, P.R., and Shapiro, M.L. (2011). Memory-guided learning: CA1 and CA3 neuronal ensembles differentially encode the commonalities and differences between situations. *J. Neurosci.* *31*, 12270–12281.
- Bakker, A., Kirwan, C.B., Miller, M., and Stark, C.E.L. (2008). Pattern separation in the human hippocampal CA3 and dentate gyrus. *Science* *319*, 1640–1642.
- Balderas, I., Rodriguez-Ortiz, C.J., Salgado-Tonda, P., Chavez-Hurtado, J., McGaugh, J.L., and Bermudez-Rattoni, F. (2008). The consolidation of object and context recognition memory involve different regions of the temporal lobe. *Learn. Mem.* *15*, 618–624.
- Buckmaster, C.A., Eichenbaum, H., Amaral, D.G., Suzuki, W.A., and Rapp, P.R. (2004). Entorhinal cortex lesions disrupt the relational organization of memory in monkeys. *J. Neurosci.* *24*, 9811–9825.
- Bunsey, M., and Eichenbaum, H. (1996). Conservation of hippocampal memory function in rats and humans. *Nature* *379*, 255–257.
- Colgin, L.L., Leutgeb, S., Jezek, K., Leutgeb, J.K., Moser, E.I., McNaughton, B.L., and Moser, M.-B. (2010). Attractor-map versus autoassociation based attractor dynamics in the hippocampal network. *J. Neurophysiol.* *104*, 35–50.
- Davachi, L., Mitchell, J.P., and Wagner, A.D. (2003). Multiple routes to memory: distinct medial temporal lobe processes build item and source memories. *Proc. Natl. Acad. Sci. USA* *100*, 2157–2162.
- Deadwyler, S.A., Bunn, T., and Hampson, R.E. (1996). Hippocampal ensemble activity during spatial delayed-nonmatch-to-sample performance in rats. *J. Neurosci.* *16*, 354–372.
- Deng, W., Mayford, M., and Gage, F.H. (2013). Selection of distinct populations of dentate granule cells in response to inputs as a mechanism for pattern separation in mice. *Elife* *2*, e00312.
- Deshmukh, S.S., and Knierim, J.J. (2013). Influence of local objects on hippocampal representations: Landmark vectors and memory. *Hippocampus* *23*, 253–267.
- Devito, L.M., Kanter, B.R., and Eichenbaum, H. (2010). The hippocampus contributes to memory expression during transitive inference in mice. *Hippocampus* *20*, 208–217.
- Diana, R.A., Yonelinas, A.P., and Ranganath, C. (2007). Imaging recollection and familiarity in the medial temporal lobe: a three-component model. *Trends Cogn. Sci.* *11*, 379–386.
- Diana, R.A., Yonelinas, A.P., and Ranganath, C. (2010). Medial temporal lobe activity during source retrieval reflects information type, not memory strength. *J. Cogn. Neurosci.* *22*, 1808–1818.
- Dupret, D., O'Neill, J., Pleydell-Bouverie, B., and Csicsvari, J. (2010). The reorganization and reactivation of hippocampal maps predict spatial memory performance. *Nat. Neurosci.* *13*, 995–1002.
- Dusek, J.A., and Eichenbaum, H. (1997). The hippocampus and memory for orderly stimulus relations. *Proc. Natl. Acad. Sci. USA* *94*, 7109–7114.
- Eichenbaum, H. (2004). Hippocampus: cognitive processes and neural representations that underlie declarative memory. *Neuron* *44*, 109–120.
- Eichenbaum, H., Kuperstein, M., Fagan, A., and Nagode, J. (1987). Cue-sampling and goal-approach correlates of hippocampal unit activity in rats performing an odor-discrimination task. *J. Neurosci.* *7*, 716–732.
- Eichenbaum, H., Yonelinas, A.P., and Ranganath, C. (2007). The medial temporal lobe and recognition memory. *Annu. Rev. Neurosci.* *30*, 123–152.
- Farovik, A., Dupont, L.M., and Eichenbaum, H. (2010). Distinct roles for dorsal CA3 and CA1 in memory for sequential nonspatial events. *Learn. Mem.* *17*, 12–17.
- Gilbert, P.E., Kesner, R.P., and DeCoteau, W.E. (1998). Memory for spatial location: role of the hippocampus in mediating spatial pattern separation. *J. Neurosci.* *18*, 804–810.
- Greene, A.J., Gross, W.L., Elsinger, C.L., and Rao, S.M. (2006). An fMRI analysis of the human hippocampus: inference, context, and task awareness. *J. Cogn. Neurosci.* *18*, 1156–1173.
- Hasselmo, M.E., and Wyble, B.P. (1997). Free recall and recognition in a network model of the hippocampus: simulating effects of scopolamine on human memory function. *Behav. Brain Res.* *89*, 1–34.
- Hayman, R.M.A., Chakraborty, S., Anderson, M.I., and Jeffery, K.J. (2003). Context-specific acquisition of location discrimination by hippocampal place cells. *Eur. J. Neurosci.* *18*, 2825–2834.
- Heckers, S., Zalesak, M., Weiss, A.P., Ditman, T., and Titone, D. (2004). Hippocampal activation during transitive inference in humans. *Hippocampus* *14*, 153–162.
- Hoge, J., and Kesner, R.P. (2007). Role of CA3 and CA1 subregions of the dorsal hippocampus on temporal processing of objects. *Neurobiol. Learn. Mem.* *88*, 225–231.
- Holdstock, J.S., Mayes, A.R., Roberts, N., Cezayirli, E., Isaac, C.L., O'Reilly, R.C., and Norman, K.A. (2002). Under what conditions is recognition spared relative to recall after selective hippocampal damage in humans? *Hippocampus* *12*, 341–351.
- Howard, M.W., and Kahana, M.J. (2002). A distributed representation of temporal context. *J. Math. Psychol.* *46*, 269–299.
- Komorowski, R.W., Manns, J.R., and Eichenbaum, H. (2009). Robust conjunctive item-place coding by hippocampal neurons parallels learning what happens where. *J. Neurosci.* *29*, 9918–9929.
- Komorowski, R.W., Garcia, C.G., Wilson, A., Hattori, S., Howard, M.W., and Eichenbaum, H. (2013). Ventral hippocampal neurons are shaped by experience to represent behaviorally relevant contexts. *J. Neurosci.* *33*, 8079–8087.
- Kreiman, G., Koch, C., and Fried, I. (2000). Category-specific visual responses of single neurons in the human medial temporal lobe. *Nat. Neurosci.* *3*, 946–953.

- Kriegeskorte, N., Mur, M., and Bandettini, P. (2008). Representational similarity analysis - connecting the branches of systems neuroscience. *Front. Syst. Neurosci.* 2, 4.
- Kubie, J., and Ranck, J. (1983). Sensory-behavioral correlates in individual hippocampus neurons in three situations: Space and context. In *Neurobiology of the Hippocampus*, W. Seifert, ed. (San Diego: Academic Press), pp. 303–319.
- Kumaran, D., Summerfield, J.J., Hassabis, D., and Maguire, E.A. (2009). Tracking the emergence of conceptual knowledge during human decision making. *Neuron* 63, 889–901.
- Kumaran, D., Melo, H.L., and Duzel, E. (2012). The emergence and representation of knowledge about social and nonsocial hierarchies. *Neuron* 76, 653–666.
- Lee, I., Yoganarasimha, D., Rao, G., and Knierim, J.J. (2004). Comparison of population coherence of place cells in hippocampal subfields CA1 and CA3. *Nature* 430, 456–459.
- Leutgeb, S., Leutgeb, J.K., Treves, A., Moser, M.-B., and Moser, E.I. (2004). Distinct ensemble codes in hippocampal areas CA3 and CA1. *Science* 305, 1295–1298.
- Leutgeb, S., Leutgeb, J.K., Barnes, C.A., Moser, E.I., McNaughton, B.L., and Moser, M.-B. (2005). Independent codes for spatial and episodic memory in hippocampal neuronal ensembles. *Science* 309, 619–623.
- Mankin, E.A., Sparks, F.T., Slayyeh, B., Sutherland, R.J., Leutgeb, S., and Leutgeb, J.K. (2012). Neuronal code for extended time in the hippocampus. *Proc. Natl. Acad. Sci. USA* 109, 19462–19467.
- Manns, J.R., and Eichenbaum, H. (2009). A cognitive map for object memory in the hippocampus. *Learn. Mem.* 16, 616–624.
- Markus, E.J., Qin, Y.L., Leonard, B., Skaggs, W.E., McNaughton, B.L., and Barnes, C.A. (1995). Interactions between location and task affect the spatial and directional firing of hippocampal neurons. *J. Neurosci.* 15, 7079–7094.
- McClelland, J.L. (2013). Incorporating rapid neocortical learning of new schema-consistent information into complementary learning systems theory. *J. Exp. Psychol. Gen.* 142, 1190–1210.
- McClelland, J.L., McNaughton, B.L., and O'Reilly, R.C. (1995). Why there are complementary learning systems in the hippocampus and neocortex: insights from the successes and failures of connectionist models of learning and memory. *Psychol. Rev.* 102, 419–457.
- McKenzie, S., and Eichenbaum, H. (2011). Consolidation and reconsolidation: two lives of memories? *Neuron* 71, 224–233.
- McKenzie, S., Robinson, N.T.M., Herrera, L., Churchill, J.C., and Eichenbaum, H. (2013). Learning causes reorganization of neuronal firing patterns to represent related experiences within a hippocampal schema. *J. Neurosci.* 33, 10243–10256.
- Moita, M.A.P., Rosis, S., Zhou, Y., LeDoux, J.E., and Blair, H.T. (2003). Hippocampal place cells acquire location-specific responses to the conditioned stimulus during auditory fear conditioning. *Neuron* 37, 485–497.
- Norman, K.A. (2010). How hippocampus and cortex contribute to recognition memory: revisiting the complementary learning systems model. *Hippocampus* 20, 1217–1227.
- Norman, K.A., and O'Reilly, R.C. (2003). Modeling hippocampal and neocortical contributions to recognition memory: a complementary-learning-systems approach. *Psychol. Rev.* 110, 611–646.
- O'Keefe, J. (1999). Do hippocampal pyramidal cells signal non-spatial as well as spatial information? *Hippocampus* 9, 352–364.
- Parkinson, J.K., Murray, E.A., and Mishkin, M. (1988). A selective mnemonic role for the hippocampus in monkeys: memory for the location of objects. *J. Neurosci.* 8, 4159–4167.
- Paz-Villagrán, V., Save, E., and Poucet, B. (2004). Independent coding of connected environments by place cells. *Eur. J. Neurosci.* 20, 1379–1390.
- Piaget, J. (1928). *Judgment and Reasoning in the Child*. (London: Kegan, Paul, Trench, and Trubner).
- Poppenk, J., McIntosh, A.R., Craik, F.I.M., and Moscovitch, M. (2010). Past experience modulates the neural mechanisms of episodic memory formation. *J. Neurosci.* 30, 4707–4716.
- Preston, A.R., Shrager, Y., Dudukovic, N.M., and Gabrieli, J.D.E. (2004). Hippocampal contribution to the novel use of relational information in declarative memory. *Hippocampus* 14, 148–152.
- Quiroga, R.Q., Reddy, L., Kreiman, G., Koch, C., and Fried, I. (2005). Invariant visual representation by single neurons in the human brain. *Nature* 435, 1102–1107.
- Rigotti, M., Barak, O., Warden, M.R., Wang, X.-J., Daw, N.D., Miller, E.K., and Fusi, S. (2013). The importance of mixed selectivity in complex cognitive tasks. *Nature* 497, 585–590.
- Rolls, E.T. (2013). A quantitative theory of the functions of the hippocampal CA3 network in memory. *Front Cell Neurosci* 7, 98.
- Ross, D.A., McGugin, R.W., and Gauthier, I. (2014). Heterogeneity of FFA responses or multiplexing? *Trends Cogn. Sci.* 18, 171–172.
- Shohamy, D., and Wagner, A.D. (2008). Integrating memories in the human brain: hippocampal-midbrain encoding of overlapping events. *Neuron* 60, 378–389.
- Singer, A.C., Karlsson, M.P., Nathe, A.R., Carr, M.F., and Frank, L.M. (2010). Experience-dependent development of coordinated hippocampal spatial activity representing the similarity of related locations. *J. Neurosci.* 30, 11586–11604.
- Spies, H.J., Hayman, R.M.A., Jovalekic, A., Marozzi, E., and Jeffery, K.J. (2013). Place Field Repetition and Purely Local Remapping in a Multicompartment Environment. *Cereb. Cortex*. Published online August 13, 2013. <http://dx.doi.org/10.1093/cercor/bht198>.
- Thompson, L.T., and Best, P.J. (1990). Long-term stability of the place-field activity of single units recorded from the dorsal hippocampus of freely behaving rats. *Brain Res.* 509, 299–308.
- Tse, D., Langston, R.F., Kakeyama, M., Bethus, I., Spooner, P.A., Wood, E.R., Witter, M.P., and Morris, R.G.M. (2007). Schemas and memory consolidation. *Science* 316, 76–82.
- van Kesteren, M.T.R., Fernández, G., Norris, D.G., and Hermans, E.J. (2010). Persistent schema-dependent hippocampal-neocortical connectivity during memory encoding and postencoding rest in humans. *Proc. Natl. Acad. Sci. USA* 107, 7550–7555.
- van Kesteren, M.T.R., Rüter, D.J., Fernández, G., and Henson, R.N. (2012). How schema and novelty augment memory formation. *Trends Neurosci.* 35, 211–219.
- Vargha-Khadem, F., Gadian, D.G., Watkins, K.E., Connelly, A., Van Paesschen, W., and Mishkin, M. (1997). Differential effects of early hippocampal pathology on episodic and semantic memory. *Science* 277, 376–380.
- Vazdarjanova, A., and Guzowski, J.F. (2004). Differences in hippocampal neuronal population responses to modifications of an environmental context: evidence for distinct, yet complementary, functions of CA3 and CA1 ensembles. *J. Neurosci.* 24, 6489–6496.
- Wiebe, S.P., and Stäubli, U.V. (1999). Dynamic filtering of recognition memory codes in the hippocampus. *J. Neurosci.* 19, 10562–10574.
- Wills, T.J., Lever, C., Cacucci, F., Burgess, N., and O'Keefe, J. (2005). Attractor dynamics in the hippocampal representation of the local environment. *Science* 308, 873–876.
- Wimmer, G.E., and Shohamy, D. (2012). Preference by association: how memory mechanisms in the hippocampus bias decisions. *Science* 338, 270–273.
- Witter, M.P., Wouterlood, F.G., Naber, P.A., and Van Haeften, T. (2000). Anatomical organization of the parahippocampal-hippocampal network. *Ann. N Y Acad. Sci.* 911, 1–24.
- Wood, E.R., Dudchenko, P.A., and Eichenbaum, H. (1999). The global record of memory in hippocampal neuronal activity. *Nature* 397, 613–616.

Xu, W., and Südhof, T.C. (2013). A neural circuit for memory specificity and generalization. *Science* 339, 1290–1295.

Yassa, M.A., and Stark, C.E.L. (2011). Pattern separation in the hippocampus. *Trends Neurosci.* 34, 515–525.

Zeithamova, D., and Preston, A.R. (2010). Flexible memories: differential roles for medial temporal lobe and prefrontal cortex in cross-episode binding. *J. Neurosci.* 30, 14676–14684.

Zeithamova, D., Dominick, A.L., and Preston, A.R. (2012). Hippocampal and ventral medial prefrontal activation during retrieval-mediated learning supports novel inference. *Neuron* 75, 168–179.

Ziv, Y., Burns, L.D., Cocker, E.D., Hamel, E.O., Ghosh, K.K., Kitch, L.J., El Gamal, A., and Schnitzer, M.J. (2013). Long-term dynamics of CA1 hippocampal place codes. *Nat. Neurosci.* 16, 264–266.

Neuron, Volume 83

Supplemental Information

**Hippocampal Representation of Related
and Opposing Memories Develop within Distinct,
Hierarchically Organized Neural Schemas**

Sam McKenzie, Andrea J. Frank, Nathaniel R. Kinsky, Blake Porter, Pamela D. Rivière,
and Howard Eichenbaum

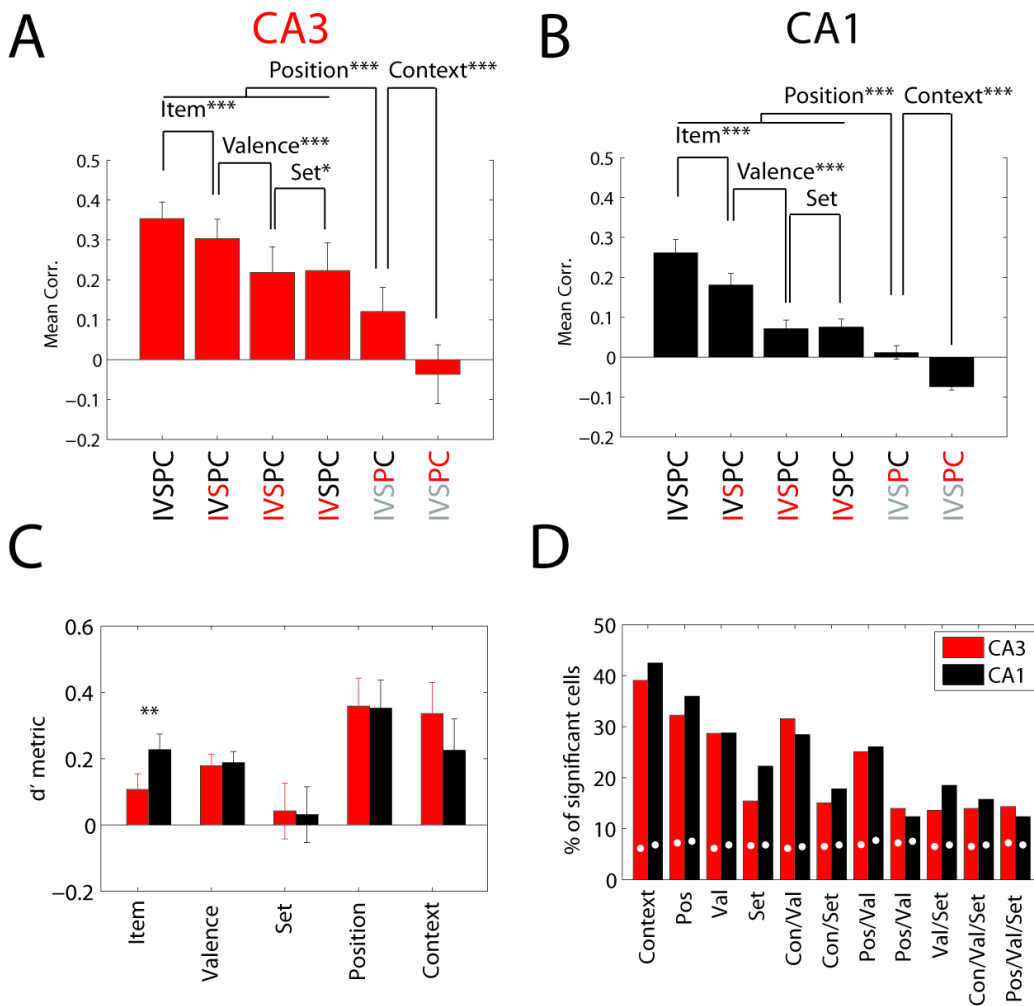


Figure S1 related to Figure 3. Comparison of CA1 (N = 292) and CA3 (N = 279). For CA3 (A) and CA1 (B) the average correlations for within- and between-condition trials are shown for each task dimension (see Table 1). IVSPC is an acronym for each task dimension: Item (I), Valence (V), Set (S), Position (P), Context (C). Black lettering indicates that trials were correlated within the same condition for that context (e.g. correlation of trials within Position 1). Red lettering indicates that correlations were taken from trials between conditions (e.g. correlation of ensembles from trials in Position 1 with those in Position 2). Grey lettering indicates correlation both within and between conditions for that dimension. For all dimensions except set in CA1, the correlations are higher for within condition trials than between. The error bars are SEM for the 9 CA1 and 11 CA3 sessions. (C) The d' metric for each task dimension for CA3 (red) and CA1 (black). Item coding within a position was greater in CA1 than in CA3. Error bars show the confidence intervals from the bootstrap analysis in which region labels were shuffled (D) The proportion of cells whose firing rates were significantly ($p < 0.05$) modulated by each main effect (Context, Position, Valence, Set) and the interaction between factors in the 4-way ANOVA. The interaction between valence and item set (Val/Set) reflects item coding. White dots within each bar mark the 95% confidence interval for each proportion ($\sim 6-7\%$) as calculated from a data set in which trial identities were shuffled 1000 times. Equal proportions were observed in CA1 and CA3. * = $p < 0.05$, *** = $p < 0.0001$.

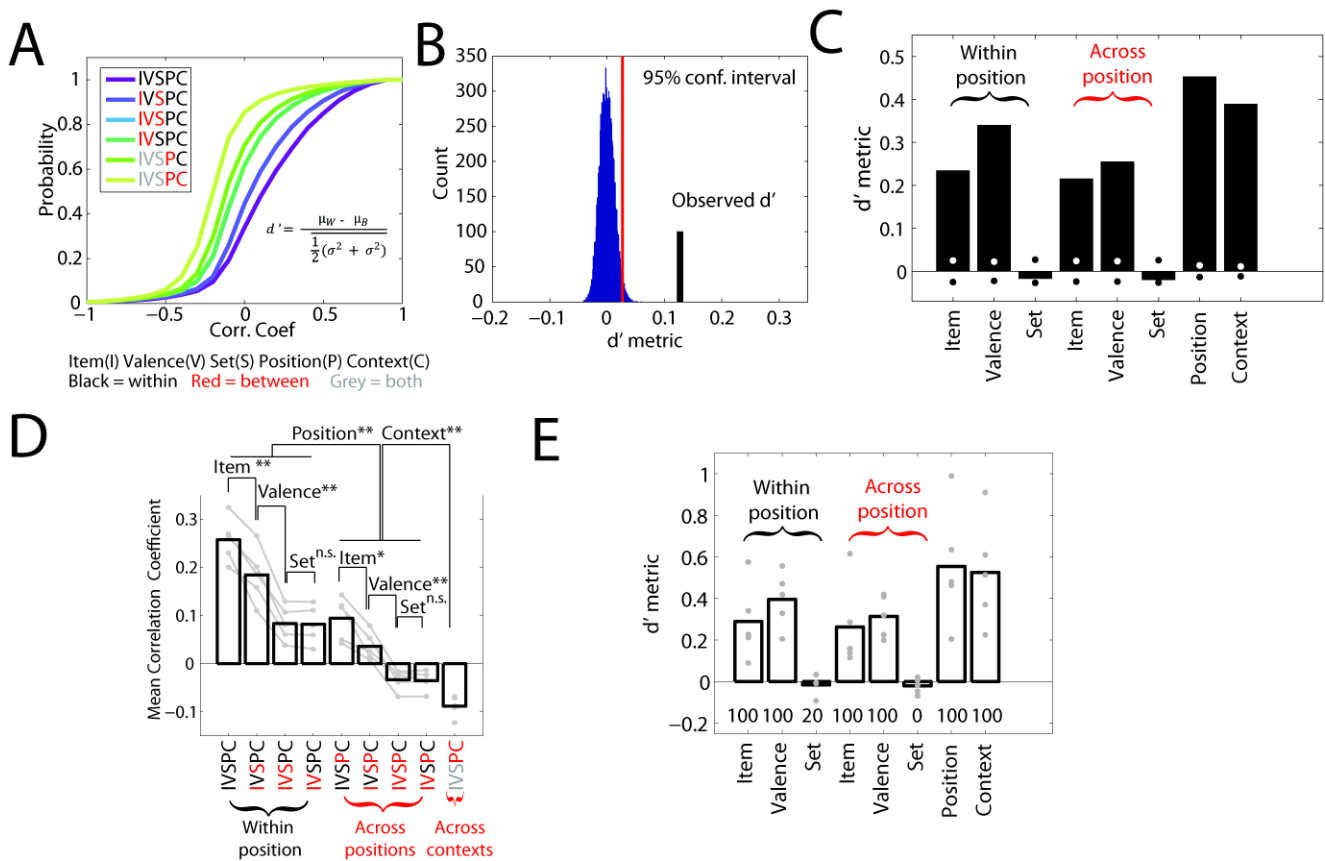


Figure S2 related to Figure 3. (A) The cumulative distribution function of ensemble correlations recorded during trials with varying degrees of overlap in the identity and position of the sampled item. IVSPC as defined in Figure S1. Distributions were compared with a d' metric. (B) The item and position labels for each trial were randomly shuffled 10000 times and the d' metric specifying the degree of dimensional coding for each of shuffled data set. The observed d' was then compared to the distribution calculated from the bootstrapped data. (C) The d' values for each dimension calculated from data pooled across sessions. The dots centered around zero indicate the 95% confidence intervals for each dimension calculated from the bootstrap analysis with data pooled from all sessions. Note that the observed d' metrics for set coding within a position (Set/Pos) and across positions (Set/xPos) fail to exceed chance values, though each other d' metric falls far beyond the values calculated from the bootstrap analysis. (D) The average correlation coefficients as shown in Figure 3D with individual rat correlations plotted for each task dimension. Significance testing was additionally conducted using paired t-tests ($N = 5$) on the Fisher transform of each correlation coefficient. The significance of each dimension was the same irrespective of whether hypothesis testing was done using the bootstrap method or the parametric comparison of the means. Additionally, one way t-tests showed that each condition was significantly ($p < 0.05$) different from zero except the correlation of ensembles recorded on samples in different positions with different items of the same valence ($p = 0.053$). (E) The mean of the each rat's d' metric. Numbers above each bar indicate the percentage of rats ($N = 5$) for which within session bootstrap significance testing yielded significant ($p < 0.05$) coding of that task dimension. The one rat with significant set coding (Set/Pos) showed higher correlations for items of the *opposite* set. * $p < .05$, ** $p < 0.01$.

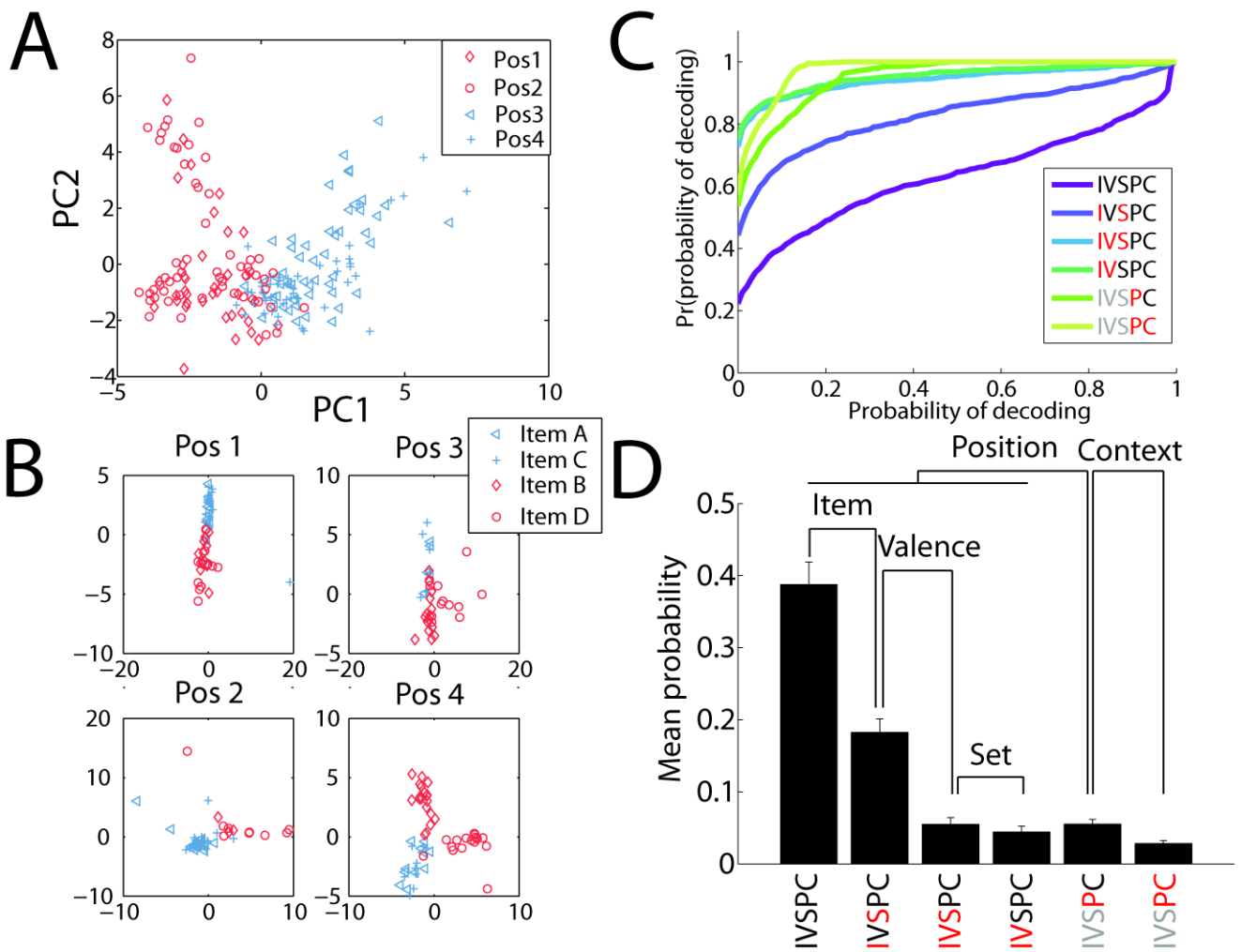


Figure S3 related to Figure 3. (A) The principal component representation of every trial from one session (ABCD2) for one rat projected onto the first two PC axes. Context 1 = red, Context 2 = blue. Pos1 = \diamond , Pos2 = \circ , Pos 3 = Δ , Pos 4 = $+$. Note how ensemble representation from the same positions and contexts cluster. (B) Each subplot shows the trials in one location plotted onto the first two PC axes for that position. Color shows different valence, marker shows different items. Valence difference is evident by color separation in Positions 1 and 4. Item difference is shown by clustering of circles and diamonds in Position 4, for example. (C) The cumulative probability function of a Bayesian classifier estimating the probability that an ensemble was recorded in response to the same or different conditions from which the data was actually recorded. (D) The mean probability associated with decoding a trial to different item and place conjunctions that were the same and/or different as that in which the data was collected. The probability of classification to trials of the same condition was greater than classification between conditions within that dimension for: context, position, valence and item but not set. These results are qualitatively similar as those found using correlation coefficients. Color coded IVSPC as in Figure S1, black = decoded from same condition, red = decoded from different dimensions, grey = average of same and different.

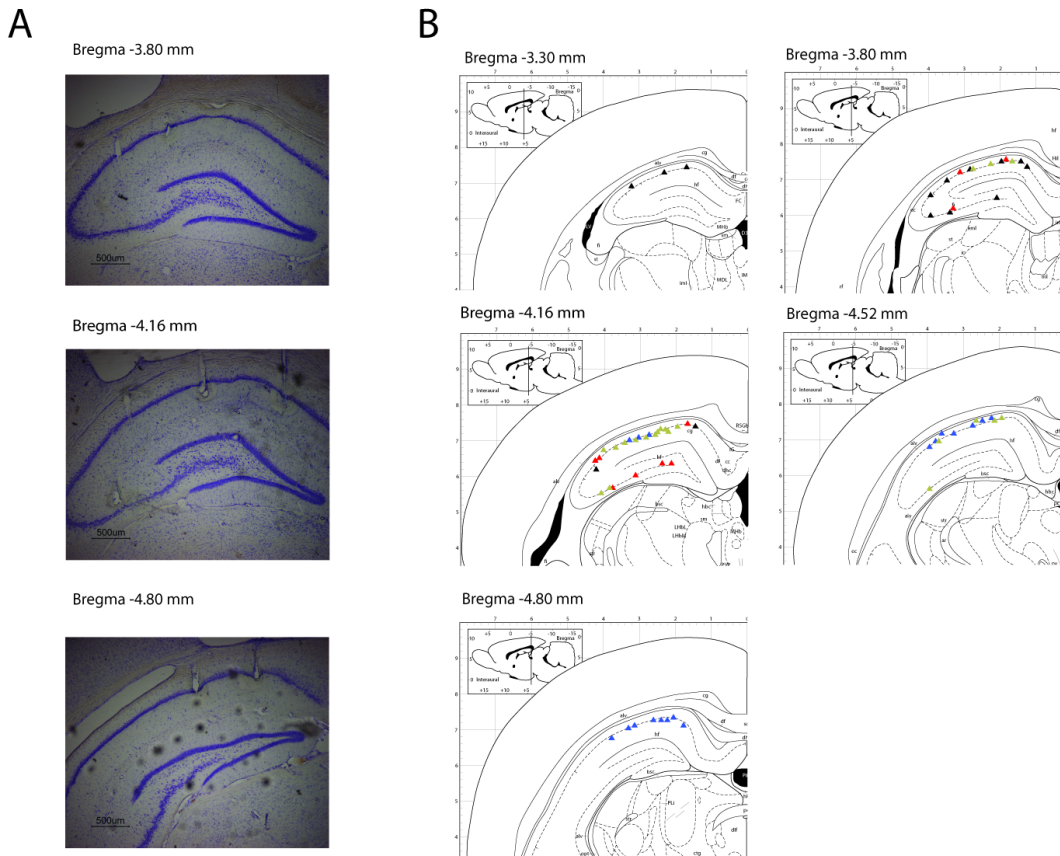
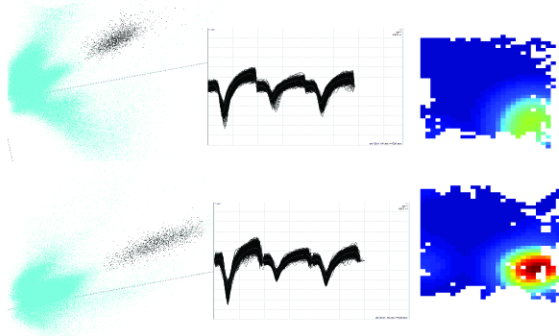
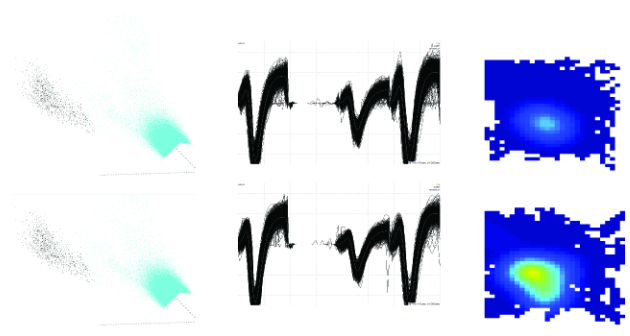


Figure S4 related to Figures 2. (A) *Top* Two tetrode lesion tracks in CA1 *Middle* Three lesion marks in CA1 and one in CA3 *Bottom* Two lesion marks in CA1. (B) The distribution of all identified lesion marks color coded by rat (n=4). Histology from one rat was damaged when the drive was removed.

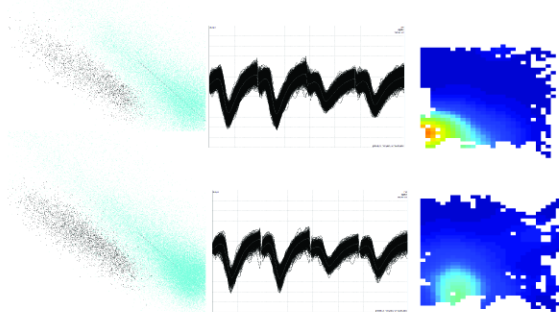
waveform corr. = 0.908, L-ratio = 4.14^{-4} , rate map corr. = 0.93



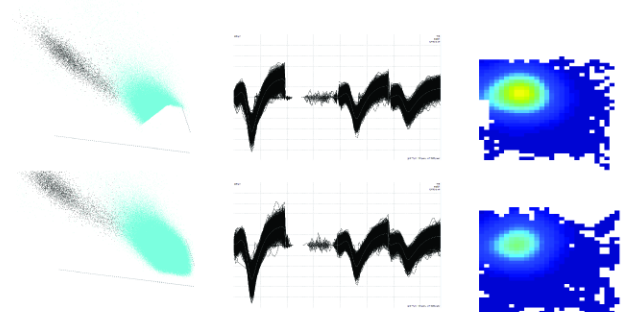
waveform corr. = 0.995, L-ratio = 7.24^{-5} , rate map corr. = 0.88



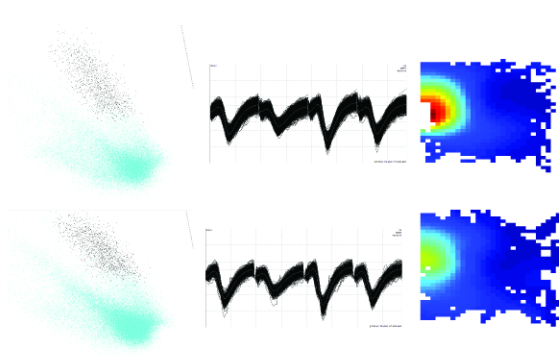
waveform corr. = 0.987, L-ratio = 0.015, rate map corr. = 0.83



waveform corr. = 0.988, L-ratio = 0.016, rate map corr. = 0.90



waveform corr. = 0.994, L-ratio = 0.005, rate map corr. = 0.93



waveform corr. = 0.995, L-ratio = 2.01^{-4} , rate map corr. = 0.89

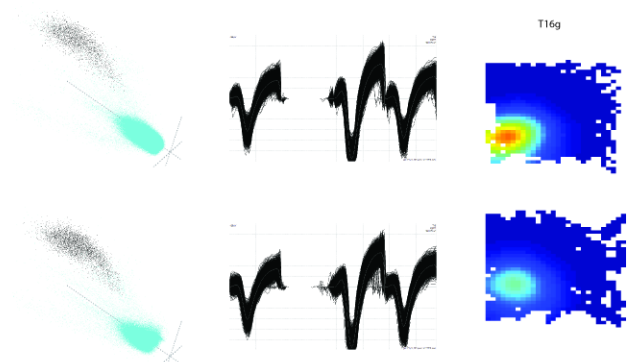


Figure S5 related to Figure 5. Stability analysis for six cells. For each cell on the right is shown the waveforms of that unit (black) and the noise (light blue) plotted according to peak-valley on three of the four electrodes for two sessions (AB3 and CD1) separated by 24 hours. The center plot shows the waveforms for those cells recorded during the two sessions. On the right shows the place fields for the same cell recorded during two explorations of an open field separated by 24 hours.

Supplemental Experimental Procedures

Surgery

Rats were anesthetized using a mixture of 3% isoflurane in oxygen and were injected with atropine (0.03 mg/kg, s.c.) and buprenorphine (0.1 mg/kg, s.c.) before surgery and meloxicam (1 mg/kg, s.c.) immediately after surgery. An ophthalmic ointment was applied to the eyes, and temperature was maintained between 36°C and 38°C. Ringer's solution was injected to maintain hydration. Stainless steel bone screws, including two ground screws over the cerebellum, were inserted into the skull. A 2.0-mm-diameter hole was drilled into the skull using a dental drill, and the dura was removed. The base of the microdrive was aimed at the CA1 and CA3 region of the right dorsal hippocampus (−3.6 mm anteroposterior, +2.9 mm mediolateral). The craniotomy was sealed with Kwik Sil (World Precision Instruments), the microdrive and ground wires were secured in place using dental acrylic (Henry Schein), and the surgical site was sutured shut.

Electrophysiological recordings

Individually movable 24-tetrode microdrives were built in-house. Tetrodes were spun from four nichrome wires (12.5 μm diameter; California Fine Wire, Grover Beach, CA, USA) and gold plated for an impedance of 200 kΩ at 1 kHz. At the end of surgery, each tetrode was lowered ~850 μm into the brain. After 5 d of recovery, the tetrodes were lowered further over 7–14 d toward the CA1 and CA3 pyramidal cell layers. After the experiments, 25 μA of current was passed through each tetrode for 30 s before perfusion and histological confirmation of tetrode placement.

As reported previously (McKenzie et al., 2013) the electrical signal was referenced to a common skull screw and differentially filtered for single-unit activity (154 Hz to 8.8 kHz). The amplified spikes from each wire were digitized at 40 kHz, and monitored with the Multineuron Acquisition Processor (Plexon). Individual pyramidal neurons were isolated using Offline Sorter (Plexon) by visualizing combinations of waveform features (peak valley, valley, peak, principal components, nonlinear energy and timestamps) extracted from wires making up a single tetrode (i.e., “manual cluster cutting”). Single-neuron selectivity was verified by the interspike interval histograms that contained no successive spikes within a 2 ms refractory period.

Apparatus.

The apparatus consisted of two wooden chambers connected by an alleyway. Each chamber was 40.6 x 40.6 x 43cm. The central alley connecting the chambers was 40.6cm long. Scented terra cotta pots could be positioned in two locations 30cm apart within each context at the corners of the context on the opposite side of the central alleyway. Four contexts were used in the study, two in each chamber; each had inserts on the walls and floor with unique texture and color. For shaping and pre-training, Context 0 was Clear Plastic taped to the wood chamber and Context 00 was Green Foam Strips taped to the wood. During the training, two new contexts were used in the same chambers: Context 1 was black anti-static cloth and Context 2 was white sand paper.

Items were terracotta pots (diameter:10.2cm, height:10.2cm) weighted with sand, capped with melted wax, filled with different digging media (3cm deep), and scented with essential oils mixed with Crisco around the rim. Scent concentration was calibrated for human just-noticeable-detection. Two items were used for pre-training: Item X (medium: purple plastic beads, scent: banana) and Item Y (medium: shredded paper, scent: hazelnut). Four different items were used for training: Item A (scent: geranium, medium: multicolored triangle foam pieces), Item B (scent: maple, medium: gravel), Item C (scent: raspberry, medium: 1cm cut red coffee stirrers), and Item D (scent: cinnamon, medium: blue rubber mulch).

Behavioral Training.

Habituation and Shaping: Ten male Long-Evans rats were maintained at 85% of their free feed body weight throughout training and testing. Rats were handled for approximately one week for 5-20 minutes daily during which point they were given Froot Loops which would later serve as motivation learning. The shaping for rats that would be implanted different slightly from that implemented for non-implanted rats.

For implanted rats ($n = 5$), on the first two habituation days, rats freely explored the apparatus with Context 0 and 00 inserts for 20 minutes with Froot Loops placed randomly throughout the environment. On the third day, Froot Loops were only placed in the corners of the two contexts where the pots would later be present (Positions 1 - 4). On the fourth day, Froot Loops were placed inside of a pot that was filled 2/3 with wax and no other digging media. The single pot could appear in any of the four locations. On subsequent days, 1/4 Froot Loop pieces were used as reward buried within the pot that was to be associated with the context during pre-training (Item X in Context 0, Item Y in Context 00).

For non-implanted rats, on the first two habituation days, rats learned to dig for buried Froot Loops in pots filled with sand in their home cage. On the third day, Froot Loops were placed inside of the same pots and rats were trained to shuttle back and forth digging in the pot for reward within the testing chambers using the pre-training contexts. Once rats reliably dug in the pots they were moved to the pre-training phase.

Pre-training. For both implanted and non-implanted rats, at the start of a trial, the rat was blocked into one chamber and allowed to explore for 10 seconds. A divider was then put down and the two pre-training items (Item X and Item Y) were placed in the corners of the chamber. The divider was lifted and the rat was free to dig in either pot. In the Context 0, Item X contained a buried reward and in Context00, Item Y contained the reward. If the rat dug (snout or paws touching the media) in the non-rewarded pot, no reward was given, both pots were quickly removed, and the trial was over. Rats were permitted to sample each pot multiple times in the absence of digging. The position of the pot (two positions per context) was pseudo-randomized for each trial such that the same item would not occur in the same location on more than two consecutive occasions. Once the rat consumed the Froot Loop, the trial ended, the alley dividers were lifted and the rat shuttled to the other context for the next trial. Every 10 trials, the rat was kept in the same context for two trials in a row to ensure that the rats did not adopt an alternating strategy. Every 10 trials, there was one trial in which no pot contained a reward to ensure behavior was not guided by the Froot Loop odor. Rats were rewarded on these trials after digging in the correct pot.

Implanted rats were given 40 trials/day which increased to 80 trials/day over 1-2 weeks. Training was carried out for approximately 3-4 weeks until the rat reached a criteria of 85% correct within a session. Once the rat reached criterion, they were scheduled for micro-drive implant surgery. After at least one week of recovery, rats were retrained on the pre-training items while tetrodes were lowered into position (up to one month of daily training).

Non-implanted rats received 40 trials/day until they performed greater than 85% correct in both contexts for two consecutive days.

Training. Training for the two cohorts was matched as closely as possible. Rats were introduced to a novel set of contexts (Context 1 and Context 2) and a new set of items (Item A and Item B). Item A was rewarded in Context 1 and Item B was rewarded in Context 2. Otherwise the task was identical to the pre-training protocol. Rats were given 75-100 trials were given per day, though more sampling events could be recorded if rats correctly rejected the non-rewarded pot (or incorrectly rejected the rewarded pot). Rats learned the reward contingencies for Item A and Item B over three days (AB1, AB2, and AB3). The day after AB3, rats were given a new item set (Item C and Item D) to be learned within the same contexts. Item C was rewarded in Context 1, Item D was rewarded in Context 2. Rats were again given 75-100 trials per day for three testing days (CD1, CD2, CD3). Rats were permitted to self correct on the first 10 trials of AB1 and CD1, though neural data collected on self-correct trials was not analyzed and only the first dig response was considered for assessment of learning.

Implanted rats continued training for three more days. The day after CD3, rats were given a block of 20 trials with only Items A and B as a reminder followed by a block of 124 trials (ABCD1) in which the rat could either receive the first item set (Item A and Item B) *or* the second item set (Item C and Item D) from one trial to the next. Items belonging to different sets were never presented on the same trial. The order in which item sets were presented was pseudo-randomized with no more than three item set repetitions in a row. The two item sets were presented inter-mixed in the same fashion for the following two days (ABCD2 and ABCD3). Data from AB1 from one rat was excluded due to experimenter error during behavioral training.

Three of the five implanted rats also completed an open field recording session after each recording session. The arena was 61x71cm and rats foraged for randomly distributed 1/4 Froot Loops for 20-30 minutes to quantify place fields in a geometrically and visually distinct environment.

Analysis

Behavioral analysis

To determine the trial in which rats reached criteria, rats were required to reach 10 out of 12 consecutive trials correct (binomial probability = 0.02) within a sliding window calculated separately for each context. The number of trials to criterion for each context was the last trial in which subjects performed less than chance. The overall trials to criteria measure was determined as the trial number on which performance was above chance in each context on two consecutive trials. The different criteria were employed because rats often developed an early strategy in which they would always dig for one item, causing higher than chance performance in one context and lower than chance performance in the other.

Single neuron analysis

We recorded from 571 units from five rats over the three overtraining days: 292 units from CA1 and another 279 cells from CA3. Based on observations during turning (e.g. passing stratum pyramidale in CA1), turn count, histology, and LFP profile (theta phase reversal between regions (Buzsaki et al., 1986) and stronger gamma in CA3 (Csicsvari et al., 2003)) cells were classified to be in either CA1 or CA3. Histology from one rat was damaged and could not be used to classify units, though in this rat all but one tetrode was directed to CA3. Removal of this rat did not alter the conclusions from any of reported findings.

Rats could sample the two items presented on each trial multiple times, and all item sampling events in which the rat dug in the rewarded pot and refrained from digging in the non-rewarded pot were considered in our analysis. To estimate the hippocampal representation of every item sampling event, for each cell the number of spikes fired was counted for up to the first 2s of item sampling and this count was divided by the sampling duration to give the average firing rate for each cell on each item sampling event.

Population analyses

The goal of the experiment was to determine how the hippocampus codes related events. In this task, events were the item sampling epochs that could be related by the following dimensions: context, position within a context, item quality, item valence, and item set. When neural activity for events that were within a condition for a particular dimension (e.g. all item sampling events in the same position) was more similar than activity recorded during events that were between conditions (e.g. events in different positions), we interpreted this as evidence for coding of that dimension within the hippocampus. The within and between conditions for each dimension are given in Table 1.

Based on firing rates from these units, two different ensemble metrics were used to measure event similarity: ensemble correlation and a naive Bayesian classifier. These methods are described below.

Ensemble Correlation. Firing rates for individual neurons were z-score normalized using the mean and standard deviation among all item sampling events to create a population vector of normalized rates for each event. The Pearson's correlation coefficient of these population vectors was calculated for every pair of events.

To calculate the strength of a coding dimension (e.g. item in position) using the ensemble correlation, we compared the average correlation for events within a condition (e.g. all item sampling events in the same position with Item A) for a task dimension (see Table 1) versus events that were between conditions for that dimension (e.g. events in the same position with Item A versus Item B) (Figure 3C, Figure S2A). For each coding dimensions, a single d' was generated either for individual rats using correlation coefficients pooled across the three sessions (Figure S2D,E) or for the experiment as a whole (Figure S2A-C) by pooling the correlations recorded in the 15 different sessions. The d' was calculated as follows:

$$d' = \frac{\mu_W - \mu_B}{\sqrt{\frac{1}{2}(\sigma_W^2 + \sigma_B^2)}}$$

where, μ_W is the mean correlation coefficient for within condition events for that dimension with variance, σ^2_W , and μ_B is the mean correlation coefficient for between condition events with variance, σ^2_B . The observed d' was compared to bootstrap data in which we randomly shuffled event identities 10000 times and then recomputed the correlation analysis and d' metric for each bootstrap sample (Figure S2B). When the observed d' was larger than 97.5% of the 10000 shuffled d' metrics, the dimension captured by the d' was considered to have been significantly coded by the hippocampus (Figure S2C).

To determine whether the distribution of correlations differed from zero, one-way d' metrics were calculated for each condition

$$d'_{oneway} = \frac{\mu_W}{\sigma_W}$$

and compared against one-way d' metrics from the shuffled data set as described above. For the shuffled data, the distributions for the one-way d' metrics were centered on zero and normally distributed.

Additional testing was done using each rat as the unit of analysis. Here, a mean correlation coefficient was calculated for each rat for each condition. Then a Fisher transform was applied to the means ($N = 5$ for each condition) and Student t-tests were used to compare conditions to one another and each condition to zero (Figure S2D).

To assess when different dimensions emerged during item sampling, we ran a similar analysis though firing rates were taken at different 250ms time bins centered $\pm 3s$ around pot sampling (Figure 4). Only events for which the rat's head remained over the pot for over 1.5s were included. Significance testing was done using the same bootstrap analysis at each time point and comparing whether the observed d' was significant at $p < 0.002$ (Bonferroni correction for 24 time points).

Bayesian Classifier

As a separate test of event similarity that had a different set of assumptions, a naive Bayesian classifier was used (MATLAB R2012b function `classify` with type set to 'diagquadratic') to determine the probability that a pattern or neural activity was recorded for each item and place combination (four items in four positions). Due to uneven sampling, rats often preferred a particular item and position combination and would sample those more often. Therefore, we only considered the last six sampling events for each item and place combination. When there were fewer than six events, that category of item and position trial was eliminated. Next, the z-scored population vector was calculated for each event, as described above. The dimensionality of the ensemble representation for each event was reduced via principal component analysis (PCA) and only the first four components were used to categorize item/position combinations (Figure S3A,B). Then, the mean, variance and covariance of each item/position four-dimensional ensemble representation was estimated with one event missing from each item and position combination. Next, a multidimensional normal distribution with the estimated means, variance and covariance matrices were fit to the each cluster of item/position ensemble representations (maximum 16). Finally, the probability of the missing events being any of the possible item/position

combinations was calculated based on the probability of that item/position combination given the ensemble representation as estimated by the normal distributions above. Since there is a probability associated with each item/position combination, we could determine whether there is hierarchy of coding probability with the correct item and place conjunction generating the highest probability, followed by correct valence, correct set, correct position, and finally correct context (Figure S3C,D).

The degree of dimensional coding was calculated in a similar fashion as that for the correlation coefficients, though the d' was calculated based on the probability of classifying within a condition or between conditions for each dimension. To test significance, we ran a bootstrap analysis in which event identities were scrambled 10000 times and if the observed d' for the difference in probabilities was greater than the 97.5% of the shuffled d' metrics, we concluded that the hippocampus coded that dimension.

Dendrogram

The hierarchical nature of the task schema was visualized using the MATLAB functions `linkage` and `dendrogram`. On days in which Items A, B, C and D were presented, the median z-score firing rates were calculated for each of the 16 item and position combinations. For each item and position combination, a large firing rate vector was created composed of the rates of every cell recorded from a session in which correct behavior was observed for every item in every position (N=560). The agglomerative hierarchical cluster tree was then created using the unweighted average distance between pairs of vectors and the Pearson's correlation coefficient as the distance metric. The nearest vector pairs were merged to form clusters. Then the nearest clusters were merged iteratively until all 16 vectors were within a single cluster (Figure 3E).

Cross-day analysis. Due to the low number of stable cells recorded in each rat, using trial by trial ensemble analyses to compare activity across testing days was not possible. Therefore, to assess the similarity of unit activity for one item set (e.g. AB) versus that for the other item set (e.g. CD), the median z-score firing rates were calculated for each of the 16 item and position combinations from both days. The z-score was calculated using the mean and standard deviation recorded for that day. As described for the dendrogram, each item and position combination (n=16) was associated with a firing rate vector composed of the rates of every cell (N=38). The pair-wise correlating of these vectors across days generated an 8x8 similarity matrix which reflects the overlap in neural activity for each item and place combination. Statistical testing was done by shuffling the item/position identity of each median rate vector and recalculating the correlations on the randomized data set.

Cell stability criteria. To determine whether the neural networks that coded the first item set (AB) were re-engaged to code related items of the second item set (CD), it was necessary to merge data across 24 hours therefore requiring assessment of recording stability. To increase the chances of stable recordings, from two days before the beginning of the experiment until the final recording day, no tetrodes were moved. Thereafter, cell stability was assessed in four ways. First, during manual cluster cutting, waveforms were viewed across time to visually confirm stability in the recording across days. Second, to quantitatively ensure high waveform stability, the average waveforms on each tetrode (four concatenated waveforms) recorded on the first day were correlated with those recorded on the second and only units with a waveform correlation greater than 0.90 were included. Next, we computed the L-ratio (Schmitzer-

Torbert et al., 2005) for the merged recording sessions using the energy of each electrode and the first principal component of the energy normalized waveform from each electrode and only accepted units with an L-ratio less than 0.08. Finally, after completing each test session three of the five rats ran for 20-30 minutes on an open field retrieving scattered food reward. Place fields were identified by calculating mean firing rate in 5x5cm bins and smoothing the binned rate map with a Gaussian kernel with $\sigma = 15\text{cm}$. Rate maps recorded across the two days were correlated, and only cells with a Pearson's correlation coefficients greater than 0.50 were retained. For the merging of AB3 with CD1, these inclusion criteria yielded 38 cells in four rats (Rat1 = 9 cells, Rat2 = 20 cells, Rat3 = 1 cell, Rat4 = 0 cells, Rat5 = 8 cells) (Figure S5).

Supplemental References

- Buzsáki, G., Czopf, J., Kondákor, I., and Kellényi, L. (1986). Laminar distribution of hippocampal rhythmic slow activity (RSA) in the behaving rat: current-source density analysis, effects of urethane and atropine. *Brain Research* 365, 125–137.
- Csicsvari, J., Jamieson, B., Wise, K.D., and Buzsáki, G. (2003). Mechanisms of gamma oscillations in the hippocampus of the behaving rat. *Neuron* 37, 311–322.
- Schmitzer-Torbert, N., Jackson, J., Henze, D., Harris, K., and Redish, A.D. (2005). Quantitative measures of cluster quality for use in extracellular recordings. *Neuroscience* 131, 1–11.